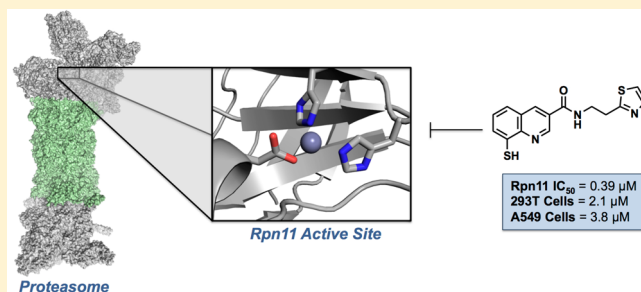


Discovery of an Inhibitor of the Proteasome Subunit Rpn11

Christian Perez,[†] Jing Li,[‡] Francesco Parlati,^{‡,⊥} Matthieu Rouffet,^{†,||} Yuyong Ma,[†] Andrew L. Mackinnon,[‡] Tsui-Fen Chou,^{‡,#} Raymond J. Deshaies,^{*,‡,§} and Seth M. Cohen^{*,†,||}[†]Department of Chemistry and Biochemistry, University of California San Diego, La Jolla, California 92093, United States[‡]Division of Biology and Biological Engineering and [§]Howard Hughes Medical Institute, California Institute of Technology, Box 114-96, Pasadena California 91107, United States

S Supporting Information

ABSTRACT: The proteasome plays a crucial role in degradation of normal proteins that happen to be constitutively or inducibly unstable, and in this capacity it plays a regulatory role. Additionally, it degrades abnormal/damaged/mutant/misfolded proteins, which serves a quality-control function. Inhibitors of the proteasome have been validated in the treatment of multiple myeloma, with several FDA-approved therapeutics. Rpn11 is a Zn²⁺-dependent metalloisopeptidase that hydrolyzes ubiquitin from tagged proteins that are trafficked to the proteasome for degradation. A fragment-based drug discovery (FBDD) approach was utilized to identify fragments with activity against Rpn11. Screening of a library of metal-binding pharmacophores (MBPs) revealed that 8-thioquinoline (8TQ, IC₅₀ value ~2.5 μM) displayed strong inhibition of Rpn11. Further synthetic elaboration of 8TQ yielded a small molecule compound (35, IC₅₀ value ~400 nM) that is a potent and selective inhibitor of Rpn11 that blocks proliferation of tumor cells in culture.



■ INTRODUCTION

Multiple myeloma (MM) is a plasma cell neoplasm that affects thousands of people each year. Currently, there is no cure for MM. Even with a strong regiment of available chemotherapies, average life expectancy from time of diagnosis ranges from 2.5 to 5 years, depending upon the stage of the disease.^{1,2} The development of novel chemotherapeutics that inhibit components of the proteasome has proven very successful in extending progression-free and overall survival.^{3,4} These drugs inhibit the ubiquitin–proteasome degradation pathway through binding to one or more of the protease active sites within the proteasome.

The ubiquitin–proteasome system (UPS) plays a major role in protein quality control by degrading unwanted, damaged, or misfolded proteins within eukaryotic cells. It also controls numerous processes including cell cycle, apoptosis, transcription, and DNA repair by modulating the stability of critical regulatory proteins. Because of the UPS playing a central role in cellular metabolism, inhibition of the proteasome has emerged as a powerful strategy for anticancer therapy. Inhibiting this pathway was validated as a clinical target with the FDA approval of bortezomib, followed by carfilzomib, and most recently ixazomib, all approved for treatment of MM. The success of these small molecules has generated substantial interest in developing inhibitors that target other key elements of the proteasome.^{5–9}

Degradation of proteins through the UPS occurs through a complex ATP-dependent pathway. Proteolysis is initiated with

the protein destined for degradation being tagged with ubiquitin. The tagged protein undergoes several rounds of ubiquitin ligation, becoming polyubiquitinated, and is then directed to the proteasome. The constitutive 26S proteasome is composed of two subcomplexes: a catalytic barrel-shaped 20S core particle (20S CP) and a 19S regulatory particle (19S RP). The 19S RP caps one or both ends of the 20S CP to form a functional 26S proteasome. Previously reported proteasome inhibitors (bortezomib, carfilzomib, and ixazomib) inhibit the proteasome by binding preferentially to the catalytic threonine residue of the β5 subunit (also known as the chymotryptic site) within the 20S CP, which is the major site of proteolysis. The polyubiquitinated protein is recognized by the 19S RP as a substrate wherein the 19S particle traps it, unfolds it, and translocates it into the 20S CP to become degraded and expelled out as oligopeptides.^{10,11} The Zn²⁺-dependent JAMM domain of the Rpn11 subunit, found within the 19S RP, cleaves ubiquitin from its substrates, thereby releasing ubiquitin for recycling. Previous reports^{12–14} demonstrate that mutations within the JAMM domain or addition of metal chelators to proteasome-dependent degradation reactions does not result in loss of substrate recognition but impairs degradation of the substrate by the proteasome because it can no longer be inserted into the 20S CP due to failure to remove the bulky ubiquitin chain, the diameter of which is wider than the entry

Received: September 20, 2016



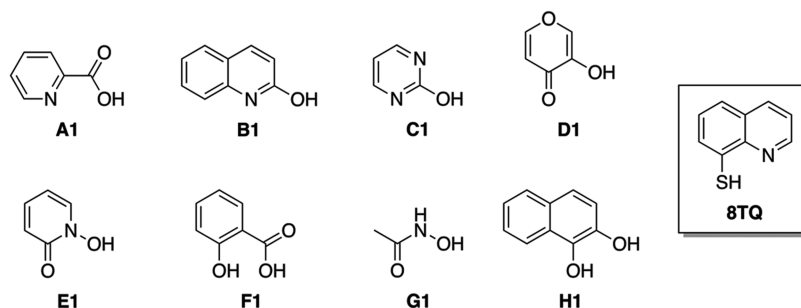


Figure 1. Representative fragments from the MBP library, including the lead fragment for this study **8TQ**.

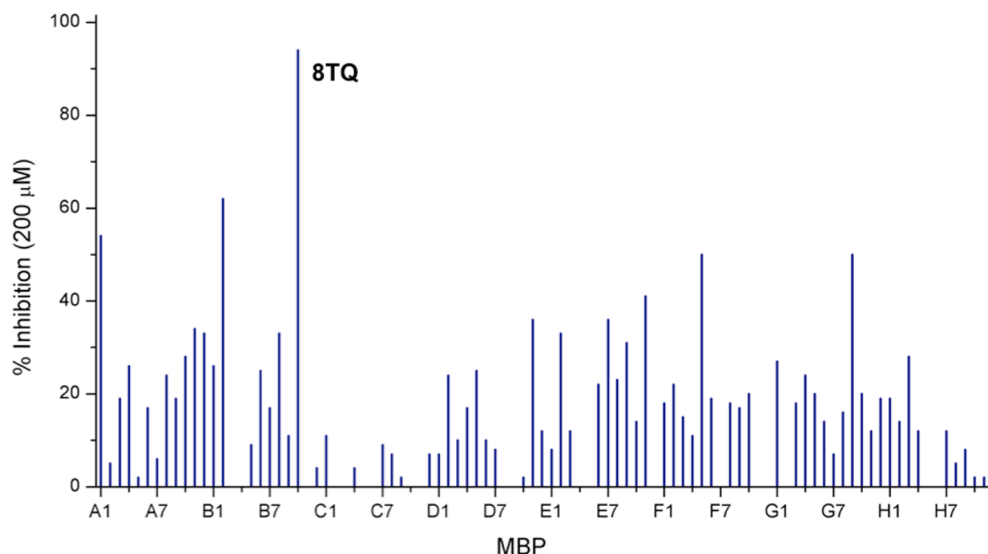


Figure 2. Plot of screening results of the MBP library against Rpn11 using a fluorescence polarization assay. Lines represent percent enzyme inhibition for a given MBP fragment at a concentration of 200 μM .

portal into the 20S CP. Inhibition of Rpn11 may lead to preferential apoptosis of neoplastic cells because these cells are thought to have a higher dependency on proteasome-dependent protein quality control compared to normal cells.^{15,16} Therefore, Rpn11 represents an attractive and novel therapeutic target for proteasome inhibition.

The catalytic JAMM motif of Rpn11 is found in seven different human proteins including the Csn5 subunit of the COP9 signalosome, AMSH, AMSH-LP, the BRCC36 subunit of BRISC, MPND, and MYSM1.^{17–23} All of these enzymes cleave the isopeptide linkage that joins ubiquitin (or the ubiquitin-like protein Nedd8 in the case of Csn5) to a second molecule of ubiquitin or to a substrate. The conserved JAMM domain has the consensus sequence $\text{EX}_n\text{HS}/\text{THX}_7\text{SXXD}$, in which the His and Asp residues bind the Zn^{2+} ion and the fourth coordination site is occupied by a water molecule that is engaged in hydrogen bonding with the conserved Glu. The Zn^{2+} acts as a Lewis acid and increases the nucleophilic character of the bound water enough to allow hydrolytic cleavage of the isopeptide bond.^{20,24}

We have employed a fragment-based drug discovery (FBDD) approach to discover inhibitors of Rpn11. The use of FBDD for the discovery of biologically active compounds has become increasingly important. This strategy consists of generating small libraries of molecular fragments and screening them against the target of interest. The hits from this screen can further be elaborated into lead compounds. Here, we report the

discovery, design, synthesis, and evaluation of a novel class of proteasome inhibitors that target Rpn11. Both a cell-free enzyme inhibition assay and a cellular assay identify Rpn11 as the target of inhibition. FBDD was utilized to identify a fragment, namely 8-thioquinoline (**8TQ**), with high affinity for the proteasome subunit Rpn11. Structure–activity relationship (SAR) experiments support the hypothesis that **8TQ** inhibits Rpn11 through coordination of its catalytic Zn^{2+} ion. SAR of the **8TQ** scaffold yielded several compounds with submicromolar potency, including a first-in-class Rpn11-selective inhibitor. The findings of the synthetic campaign described in this report prompted an extensive biological study that is described elsewhere.²⁵ This work opens the door for development of a novel class of proteasome inhibitors for cancer chemotherapy.

RESULTS

Screening of the MBP Library. The majority of previously reported proteasome inhibitors bind to the catalytic $\beta 1$, $\beta 2$, or $\beta 5$ subunits within the 20S CP,^{3,26–28} with fewer reports of inhibitors binding subunits within the 19S RP.^{29–33} An alternative approach to high-throughput screening (HTS) for the development of metalloenzyme inhibitors is through use of fragment libraries of metal-binding pharmacophores (MBPs). MBPs are small molecules that have one or more donor atoms that are capable of forming coordinate covalent bonds to the active site metal ion of metalloenzymes. To identify potent

MBPs that can serve as initial building blocks for inhibitor design, a chemical library containing 96 MBP fragments³⁴ was screened against Rpn11. The fragments are small (<300 amu) and have a known or predictable metal-binding motif (Figure 1). This MBP library has been previously used to successfully identify scaffolds for the development of several metalloenzyme inhibitors.^{35,36}

The MBP library was initially screened at a fragment concentration of 200 μM against Rpn11 by utilizing a fluorescence polarization assay.^{37,38} The fluorescence polarization assay specifically measures the deubiquitinating activity of Rpn11. The assay features a proteasome substrate with four tandem repeats of ubiquitin (Ub_4) followed by a peptide labeled with Oregon Green on a unique cysteine residue. Incubation of this substrate, $\text{Ub}_4\text{peptide}^{\text{OG}}$, with proteasome resulted in depolarization of Oregon Green fluorescence due to release of the peptide^{OG} from Ub_4 .²⁵ Initial evaluation of the MBP library revealed three compounds with >50% inhibition, with the majority of the compounds exhibiting 0–30% inhibition (Figure 2). One fragment (8TQ, Figure 1) demonstrated essentially complete inhibition at a concentration of 200 μM . Because of the particularly strong activity of 8TQ, the fragment was chosen for lead development. 8TQ was determined to have an IC_{50} value of $2.8 \pm 0.4 \mu\text{M}$, which translates to an extremely high ligand efficiency of 0.69.³⁹

As described in greater detail elsewhere,²⁵ an independent screen of >300000 compounds produced only one hit, a thioester derivative of 8TQ, which given the hydrolytic instability of the thioester group is proposed to form 8TQ as the active species. Incredibly, the results from a small MBP library screen uncovered the same privileged scaffold as a large HTS campaign, which highlight the efficiency and effectiveness of our MBP library approach to drugging metalloenzymes.

Investigating the Mechanism of Inhibition. Because of the structural similarity of 8TQ to the common metal chelator 8-hydroxyquinoline, as well as data on previously reported 8TQ metal complexes, we predicted that 8TQ would bind the catalytic Zn^{2+} ion of Rpn11 in a bidentate fashion through the endocyclic nitrogen and exocyclic sulfur donor atoms.^{40–42} To validate this hypothesis, a model was sought to allow for structural characterization of the mode of binding. Tris-(pyrazolyl)borate (Tp) complexes have been shown to serve as useful metalloenzyme active site mimics, giving some insight into bond lengths and angles for MBPs coordinated to metalloenzyme active site metal ions.^{43–48} A Zn^{2+} complex with the ligand hydrotris(5,3-methylphenylpyrazolyl)borate ($\text{Tp}^{\text{Me,Ph}}$)⁴³ was combined with 8TQ to obtain the complex $[(\text{Tp}^{\text{Me,Ph}})\text{Zn}(\text{8TQ})]$. The metal complex was readily crystallized and revealed a five-coordinate Zn^{2+} center with a trigonal bipyramidal coordination geometry (Figure 3). 8TQ was bound in the expected bidentate manner, with the sulfur donor atom positioned in the equatorial plane (2.29 Å, Zn–S distance) and the endocyclic nitrogen atom serving as an axial donor (2.17 Å, Zn–N distance). The structure of this metalloenzyme model complex supports the hypothesis that 8TQ inhibited Rpn11 by metal coordination of the active site Zn^{2+} ion.

Additional evidence for the mode of inhibition was obtained from SAR studies using 8TQ derivatives. Derivatives of 8TQ were prepared including fragments where the metal-coordinating atoms were removed, moved, or otherwise modified (Table 1). For example, compound 2 replaced the endocyclic nitrogen with a C–H group, giving a naphthyl derivative which is

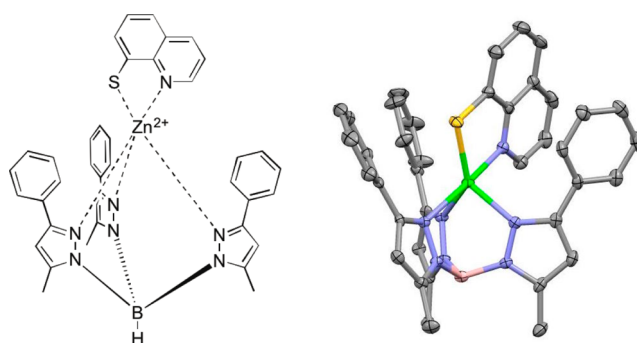


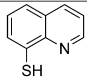
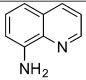
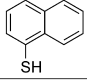
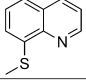
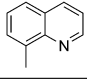
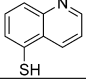
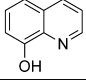
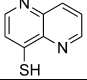
Figure 3. Chemical illustration (left) and image of the X-ray structure (right) of $[(\text{Tp}^{\text{Me,Ph}})\text{Zn}(\text{8TQ})]$. Thermal ellipsoids are shown at 50% probability. Hydrogen atoms are omitted for clarity. Color scheme: boron (pink), carbon (gray), nitrogen (blue), sulfur (yellow), and zinc (green).

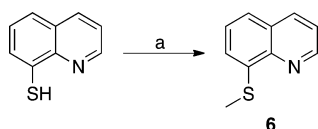
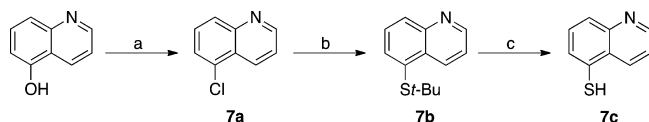
incapable of the bidentate mode of binding exhibited by 8TQ (Figure 3). Similarly, in compounds 3, 4, and 5, the thiol moiety was replaced by a methyl, hydroxyl, or amine group, respectively, giving a series of isosteric compounds that lack the requisite thiol donor atom. In compound 6, the thiol moiety was alkylated with a methyl group (Scheme 1), which prevents formation of the anionic thiolate donor atom for binding Zn^{2+} (Figure 3). Finally, compound 7c places the coordinating nitrogen atom on the opposite side of the quinoline ring from the thiol moiety (Scheme 2), which produces an isosteric compound but does not allow for bidentate binding of the ligand to the metal ion. As summarized in Table 1, compounds 2–6 and 7c all exhibited a complete loss of activity ($\text{IC}_{50} > 100 \mu\text{M}$) against Rpn11, further validating the importance of the bidentate binding of 8TQ through the nitrogen and sulfur pair of donor atoms. Further confirmation of this hypothesis was demonstrated by the activity of compound 8e, which has an additional nitrogen atom at the 5-position of the ring (Scheme 3) but otherwise can maintain the 8TQ binding motif. Compound 8e inhibits Rpn11 with an IC_{50} value of $15 \pm 3.4 \mu\text{M}$. The ~6-fold weaker activity of 8e when compared to 8TQ is attributed to the ability of 8e to tautomerize to the 1,5-naphthyridine-4(1H)-thione form.

Synthesis of Methyl Derivatives and Cross Inhibition Studies. Having established a rudimentary SAR for the requisite metal-binding features of the 8TQ scaffold, a sublibrary of 8TQ derivatives with simple modifications to the scaffold was prepared in an effort to probe for possible hydrophobic (methyl groups) contacts within the active site as well as to determine the best positions on the 8TQ ring to add substituents for subsequent rounds of derivatization. Functionalization of the 8TQ fragment was achieved largely via the Skraup and Doebner–Von Miller reactions using aniline derivatives as starting materials. Compounds 9a and 10a were synthesized starting with 2-fluoroaniline, with the quinoline ring forming upon addition of a methyl- α,β -unsaturated aldehyde in the presence of aqueous HCl (Scheme 4). The 4-methyl quinoline analogue (11a) was synthesized in similar fashion by combining 2-fluoroaniline with an α,β -unsaturated ketone (Scheme 4).

Compounds 12a and 13a were obtained by starting with methyl functionalized 2-chloro or 2-fluoroaniline in the presence of glycerol utilizing nitrobenzene as the solvent (Scheme 5). Substitution of the resulting methyl-8-fluoro or methyl-8-chloroquinolines (9a, 10a, 11a, 12a, and 13a) to

Table 1. 8TQ Fragment Derivatives Used to Examine the Role of Metal Binding in Rpn11 Inhibition

Cmpd	Structure	Rpn11 IC ₅₀ (μM)	HCT 116 Cytotoxicity (μM)	Cmpd	Structure	Rpn11 IC ₅₀ (μM)	HCT 116 Cytotoxicity (μM)
8TQ		2.8±0.36	1.6±0.7	5		>100	----
2		>100	>100	6		>100	>100
3		>100	>100	7c		>100	>100
4		>100	6	8e		15.0±3.4	----

Scheme 1. Synthesis of Compound 6^a^aCH₃I, EtOH, H₂O, 2 M NaOH, 25 °C.Scheme 2. Synthesis of Compound 7c^a^aPOCl₃, 100 °C; (b) *t*-BuSH, NaH, DMF, 140 °C; (c) 12 M HCl, 100 °C.

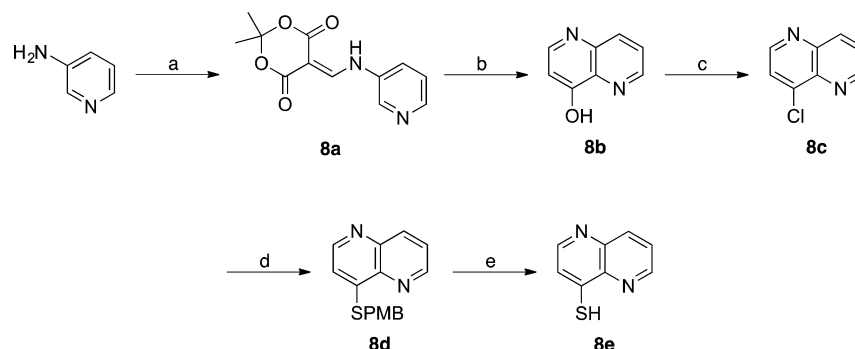
produce the thiol functionality was obtained through a nucleophilic aromatic substitution reaction utilizing *tert*-butyl thiol (*t*-BuSH). This was followed by a deprotection reaction under refluxing concentrated HCl to yield the free thiol (9c, 10c, 11c, 12c, and 13c).

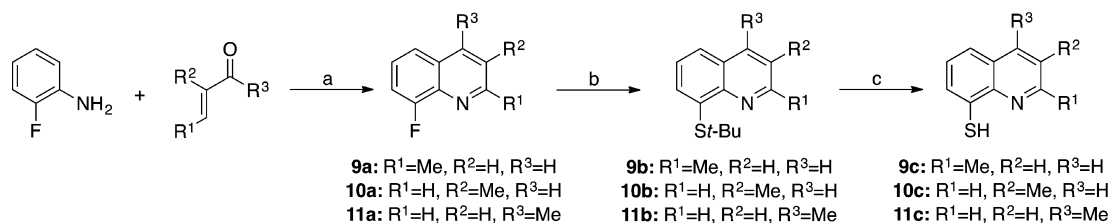
In addition to evaluation against Rpn11, the selectivity of these compounds was also examined by performing inhibition assays against a host of other metalloenzymes (Table 2). These off-target metalloenzymes were selected because they possess a diverse set of structures and functions, utilize a metal ion in a catalytic role, are clinically relevant targets, and have readily

available assays. The metalloenzymes examined included the Zn-dependent JAMM domain enzyme (Csn5), two histone deacetylases (HDAC-1, HDAC-6), a matrix metalloproteinase (MMP-2), carbonic anhydrase (hCAII), and a nonheme, Fe-dependent lipoxygenase (5-LO). In addition, to assess the effects of these compounds in a cellular model, a human colon carcinoma cell line (HCT 116) was utilized to measure the antiproliferative activity of the fragments.

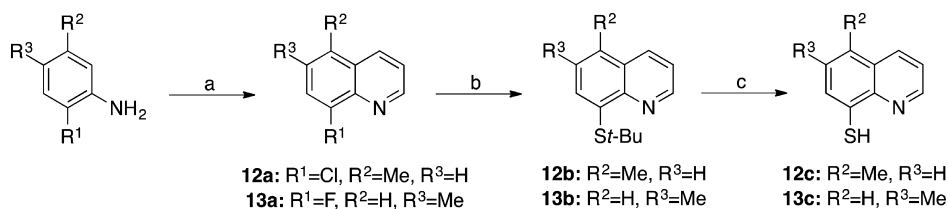
The results from these experiments are summarized in Table 2. The data demonstrate that the 8TQ scaffold was highly specific for the JAMM metalloproteins (Rpn11 and Csn5) over other metalloenzymes. Some discrimination between Rpn11 and Csn5 was observed, even with the relatively simple methyl substitutions, which suggests that specificity could be developed using this scaffold. Inhibition data also suggests that the Rpn11 active site was quite plastic and tolerated substitution at multiple positions on the 8TQ ring. Compound 9c did not inhibit the JAMM domain proteins, which correlates with loss of cytotoxicity toward the HCT 116 cell line (Table 2). Introduction of even a methyl group resulted in complete loss of activity, which suggests that functionalization at the 2-position is not tolerated.

Synthesis of an 8TQ Sublibrary. Given the high affinity of 8TQ toward JAMM domain proteins, derivatives were sought that could improve potency while also adding selectivity for Rpn11. Compounds containing functional groups at the 3- and 4-positions were primarily pursued due to the synthetic accessibility of these derivatives over other active compounds (e.g., 5- and 6-position derivatives, Table 2). In addition,

Scheme 3^a^a2,2,6-Trimethyl-4H-1,3-dioxin-4-one (Meldrum's acid), triethyl orthoformate, 105 °C; (b) Dowtherm A, 250 °C; (c) POCl₃, toluene, 110 °C; (d) (4-methoxyphenyl)methanethiol (*p*-MBSH), NaH, DMF, 25 °C; (e) *m*-cresol, TFA, reflux.

Scheme 4. Synthesis of 2-, 3-, and 4-Methyl-8-thioquinoline (Apolar) Derivatives of 8TQ^a

^aToluene, 6 M HCl, 110 °C; (b) *t*-BuSH, NaH, DMF, 140 °C; (c) 12 M HCl, 100 °C.

Scheme 5. Synthesis of 5- and 6-Methyl-8-thioquinoline^a

^aGlycerol, H₂SO₄, nitrobenzene, 150 °C; (b) *t*-BuSH, NaH, DMF, 140 °C; (c) 12 M HCl, 100 °C.

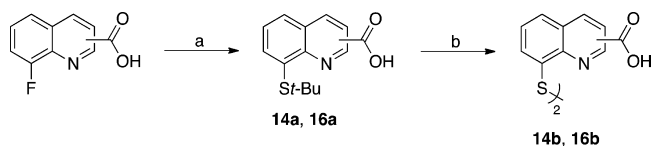
Table 2. Enzyme Inhibition Data for 8TQ and 8TQ Derivatives^a

compd	structure	Rpn11	Csn5	HDAC1	HDAC6	MMP2	5-LO	hCAII	HCT 116 cytotoxicity
8TQ	H	2.8 ± 0.4	10.3 ± 2.3	>200	>200	>200	>200	>200	1.6 ± 0.7
9c	2-Me	>100	>100	ND	ND	>200	ND	ND	>50
10c	3-Me	1.6 ± 0.6	7.1 ± 1.6	>50	>200	>200	>200	>40	2.6 ± 0.5
11c	4-Me	5.7 ± 2.0	25.1 ± 6.1	>200	>200	>200	>200	>200	>10
12c	5-Me	2.5 ± 1.3	2.9 ± 1.1	>200	>200	>200	>200	>200	3.4 ± 1.1
13c	6-Me	0.9 ± 0.3	1.6 ± 0.6	>50	>50	>200	>200	>100	2.1 ± 1.2

^aData listed includes inhibitory values against off-target metalloenzymes and cytotoxicity against the HCT 116 cell line. All IC₅₀ values listed are in μM. Reported IC₅₀ values represents the average value obtained from at least three independent measurements, with the standard deviation reported as the error.

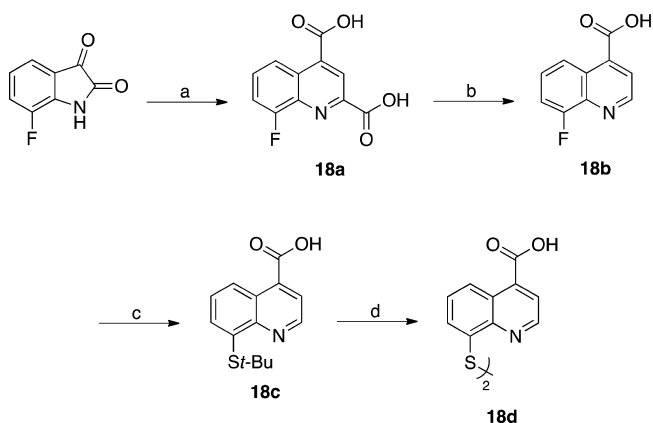
derivatives of the 2-position were prepared to confirm the SAR obtained with the methyl derivatives. Despite the good activity observed with 5- (12c) and 6- (13c) position derivatives, these were not further explored in this synthetic campaign.

Compounds 14b and 16b were synthesized starting from commercially available 2- or 3-carboxyl-8-fluoroquinoline as detailed in Scheme 6. Compound 18d was obtained via a

Scheme 6. Synthesis of 2- and 3-Carboxyl-8-thioquinoline (Polar) Derivatives^a

^a*t*-BuSH, NaH, DMF, 140 °C; (d) 12 M HCl, 110 °C.

Pfitzinger ring expansion reaction of 7-fluoroisatin and pyruvate under basic conditions to yield 18a. This was decarboxylated under aqueous conditions to afford 18b, which then yielded 18d over two steps (Scheme 7). The corresponding methyl ester derivatives were obtained via Fischer esterification (15, 17, and 19). Lastly, the 2-, 3-, and 4-carboxylate-8-thioquinoline compounds were coupled to amines mainly via the assistance of carbodiimide (CDI) or 1-[bis(dimethylamino)methylene]-1H-1,2,3-triazolo[4,5-*b*]pyridinium 3-oxide hexafluorophosphate (HATU) coupling reagents. Alkyl amines were coupled

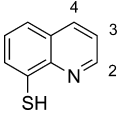
Scheme 7. Synthesis of 4-Carboxyl-8-thioquinoline^a


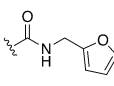
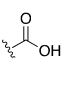
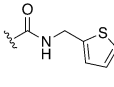
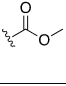
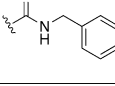
^aSodium pyruvate, 5 M NaOH, 110 °C; (b) H₂O, 170 °C; (c) *t*-BuSH, NaH, DMF, 140 °C; (d) 12 M HCl, 110 °C.

mainly through the use of CDI at room temperature; however, less nucleophilic amines (aromatic) were coupled using HATU with heating.

It should be noted that all of the aforementioned compounds were isolated as disulfide dimers, as evidenced by mass spectrometry. Under the Rpn11 assay conditions, which contained 1 mM of dithiothreitol (DTT) as a reductant, the disulfides were reduced to the monomeric active species.

Table 3. Rpn11 Inhibitory Activity of 8TQ Derivatives Functionalized at the 2-, 3-, and 4-Positions of the Ring System

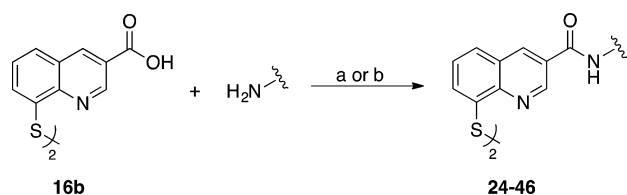


Structure	Cmpd	Position	Rpn11 IC ₅₀ (μM)	Structure	Cmpd	Position	Rpn11 IC ₅₀ (μM)
	9c	2	>100		----	2	----
	10c	3	1.6±0.6		30	3	0.9±0.1
	11c	4	5.7±2.0		23	4	2.2±0.6
	14b	2	>20		20	2	>100
	16b	3	1.1±0.1		31	3	0.8±0.3
	18d	4	1.3±0.2		22	4	1.0±0.2
	15	2	>50		21	2	>100
	17	3	0.9±0.1		39	3	1.1±0.2
	19	4	1.0±0.1		----	4	----

Screening of the aforementioned derivatives (**14b**, **15**, **20**, **21**) demonstrated that functionalization at the 2-position was not well tolerated, consistent with the findings on the simple methyl derivative (**9c**). All the compounds functionalized at the 2-position were consistently less active than **8TQ** (Table 3). In addition, activity generally decreased with increasing functional group size at the 2-position, possibly due to a clash with the protein active site.

Derivatization at the 3- and 4-positions was consistently well tolerated. To confine the scope of these initial synthetic efforts, additional exploration of derivatives was restricted to the 3-position. To accomplish this, compound **16b** was coupled to a series of amines with the assistance of CDI or HATU coupling reagents (Scheme 8). All of the compounds prepared via

Scheme 8. Synthesis of 3-Carboxamide Derivatives^a



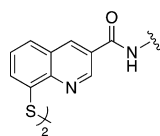
^aCDI, DMF, 25 °C; (b) HATU, Et₃N, DMF, 60 °C.

Scheme 8 were also isolated as disulfide dimers. A diverse set of amines, predominantly derivatives with substituted aryl groups or heterocycles with varying linker lengths (Table 4), was explored. To identify a potent yet selective Rpn11 inhibitor, all compounds were screened in cell-free assays against Rpn11, Csn5, and AMSH. The Rpn11 assay was carried out in the same manner in which the initial 96-fragment screen was performed. To measure Csn5 activity, a fluorescent substrate termed SCF^{SKp2}-Nedd8OG was engineered. To produce this substrate, Nedd8 containing a unique N-terminal cysteine was labeled with Oregon Green 488 and then conjugated to SCF^{SKp2} as previously described.⁴⁹ For AMSH, the substrate termed DiUB^{K63}-TAMRA was purchased from commercial sources. DiUB^{K63}-TAMRA is labeled with a FRET pair (TAMRA/QXL) that upon cleavage by AMSH produces a fluorescent signal. The SAR obtained was used to increase activity against Rpn11

while discriminating against the other JAMM domain proteins Csn5 and AMSH. In addition, a cell-based assay was utilized to measure inhibition of the proteasome in cells. For this, we utilized a HeLa cell line that stably expresses Ub^{G76V}-GFP (Green Fluorescent Protein), which serves as a fluorescent signal for proteasome activity.⁵⁰ These cells were treated with β5 inhibitor MG132 to accumulate Ub^{G76V}-GFP. The MG132 was then washed out and either DMSO or one of our compounds was added, and the decay of GFP fluorescence was monitored. Under normal conditions, the accumulated Ub^{G76V}-GFP is rapidly degraded by proteasome. However, if the proteasome function is blocked, the degradation rate of the reporter protein is reduced. The IC₅₀ values reported in Table 4 represent the concentration of test agent at which the degradation rate was reduced by half.

Evaluation of the series of compounds in Table 4 identified **28** and **35** as two promising leads. Both compounds showed submicromolar IC₅₀ values against Rpn11 in the biochemical assay and selectivity over Csn5 and AMSH. These compounds were then screened for cytotoxicity against 293T and A549 cells (Figure 4). Compound **28** had an IC₅₀ of 6.4 μM and 5.8 μM against 293T and A549 cells, respectively. Meanwhile compound **35** demonstrated slightly lower IC₅₀ values than **28** against both cell lines at 2.1 and 3.8 μM, respectively. Ultimately, compound **35** was selected as the lead compound due to its better selectivity for Rpn11 over other JAMM proteins, efficacy in the cell-based assays, and more active cytotoxic profile.

Synthesis and Evaluation of Control Compounds. A small series of control compounds (analogues of **35**) were synthesized (Schemes 9–12) to re-evaluate the role of the MBP in this lead compound. An 8-hydroxyquinoline analogue (**47**) was prepared in order to determine the importance of the softer Lewis base thiol (versus the harder Lewis base oxygen donor in 8-hydroxyquinoline). Compounds **48** and **49f** prevent metal coordination as they are elaborated analogues of inactive MBP fragments **6** and **7c** (Table 1). Similarly, compound **50f** was prepared as an elaborated analogue of the less active MBP fragment **8e**. Evaluation of these compounds yielded essentially no inhibition against Rpn11, Csn5, or AMSH (Table 5), recapitulating the SAR obtained with the original MBP fragments (Table 1).

Table 4. Inhibitory Activity against Rpn11, Csn5, and AMSH for 3-Position Substituted 8TQ Derivatives^a

Cmpd	Structure	Rpn11 IC ₅₀ (μM)	Csn5 IC ₅₀ (μM)	AMSH IC ₅₀ (μM)	UL ^{G76V} GFP Hela Cell IC ₅₀ (μM)
24	H	1.0±0.2	15.3±4.2	1.7±0.4	1.2±0.2
25	Me	1.6±0.3	68±14	4.1±1.3	2.6±0.5
26		>2	>100	2.2±0.3	>0.3
27		2.6±0.4	15±1	5.0±1.0	>10
28		0.4±0.1	20±3	4.7±1.1	1.2±0.3
29		4.6±1.4	41±5	6.8±0.5	1.0±0.2
30		0.9±0.1	<0.5	0.9±0.1	1.0±0.2
31		0.8±0.1	16±6	1.3±0.3	5.0±0.8
32		0.5±0.1	24±7	7.8±2.2	2.9±0.8
33		1.2±0.7	6.9±1.8	1.7±0.3	1.4±0.3
34		0.3±0.1	4.0±2.9	1.3±0.2	5.0±0.4
35		0.4±0.1	30±3	4.5±0.5	0.6±0.1
36		4.0±0.2	>50	17±3	>10
37		3.2±0.2	>100	3.5±0.5	>10
38		0.2±0.1	7±2	0.5±0.1	>10
39		1.1±0.1	11±4	>10	>10
40		<0.2	18±6	0.9±0.1	>10
41		0.8±0.2	>100	3.5±0.7	>10
42		<0.2	0.5±0.1	0.6±0.2	>10
43		0.9±0.2	7±1	<0.2	>10
44		0.8±0.3	0.3±0.2	0.9±0.3	>10
45		6.4±1.2	>100	26±9	>10
46		>5	>30	3.5±0.6	>10

^aCellular levels of proteasome inhibition are also listed. Reported IC₅₀ values represents the average value obtained from at least three independent measurements, with the standard deviation reported as the error.

As a final experiment to demonstrate the importance of metal coordination in this class of inhibitors, an inhibition assay was carried out utilizing compound **35** in the presence of a soluble, small molecule coordination compound Zn(cyclen)²⁺ (cyclen = 1,4,7,10-tetraazacyclododecane). In this experiment, if metal coordination is critical for the activity of compound **35** then

Zn(cyclen)²⁺ can act as a “decoy” of a Zn-metalloprotein active site, thereby titrating **35** away from Rpn11 and reducing the apparent activity of the inhibitor. When inhibition of **35** against Rpn11 was measured in the presence of Zn(cyclen)²⁺ (100 μM, Figure 5), a significant loss in activity against Rpn11 was observed (IC₅₀ = 77.4 vs 0.39 μM, Figure 5). The observed IC₅₀ value shift is attributed to the ability of Zn(cyclen)²⁺ to compete/titrate **35** away from Rpn11.

DISCUSSION

To discover a fragment that inhibits Rpn11, a FBDD approach using a 96-component library of MBPs led to the identification of the highly efficient **8TQ** fragment for inhibiting Rpn11. Upon identifying **8TQ** as an anchoring scaffold, derivatives were prepared to evaluate the hypothesis that metal binding was the source of **8TQ** activity. Indeed, the SAR obtained from compounds **2–6** and **7c** (Table 1) indicated that bidentate metal binding was essential for the observed inhibitory activity by **8TQ**. Only derivative **8e**, which possesses the same N,S donor atom set, maintains some activity against Rpn11. In addition, the bioinorganic model complex [(Tp^{Me,Ph})Zn-(**8TQ**)] clearly supports the ability of **8TQ** to form a ternary complex with a Zn²⁺ ion bound in a protein-like coordination environment (Tp^{Me,Ph}) (Figure 3). All of these results point to metal coordination as the mechanism of action for **8TQ** against Rpn11.

Upon validating the mode of inhibition by **8TQ**, efforts were made to develop a rudimentary SAR around the **8TQ** scaffold to increase activity against Rpn11 while diminishing activity toward the most prominent off-targets, namely the other JAMM family members Csn5 and AMSH. The initial strategy involved probing for hydrophobic and hydrophilic contacts near the active site while also examining steric limitations. The quinoline ring was appended with methyl groups on the 2-, 3-, 4-, 5-, and 6-positions of the ring (Scheme 4 and 5, **9c**, **10c**, **11c**, **12c**, and **13c**) or carboxylic acids on the 2-, 3-, and 4-positions of the ring (Scheme 6 and 7, **14b**, **16b**, and **18d**). Derivatives with 3- and 4-substituents, including methyl (**10c** and **11c**), carboxylate (**16b** and **18b**), and methyl ester (**17** and **19**) substituents were all well tolerated, providing a consistent SAR, while substitution at the 2-position was not as well tolerated. The behavior of carboxylate derivatives with aromatic substituents was also consistent with the observed SAR, with substituents at the 3- and 4- being well tolerated. Among these, comparing the same substituents at the 3- and 4-positions (**16b** to **18d**, **17** to **19**, and **30** to **23**) suggested that 3-position derivatives might possess marginally better activity (Table 3), and hence derivatives of the 3-position became the focus of this study.

In addition to Rpn11, active JAMM domains are found in six other human proteins: the Csn5 subunit of the COP9-signalosome, the Brcc36 subunit of the BRCC and BRISC complexes, the closely related AMSH and AMSH-LP proteins, MYSM1, and MPND. Of these, suitable biochemical assays are available for all but MYSM1 and MPND. AMSH is highly homologous to AMSH-LP, so we excluded this target from further consideration and focused our attention on Csn5 and AMSH as the major off-target concerns.⁵¹ **8TQ** showed significant inhibition of only one other JAMM domain protein (BRISC, Supporting Information, Figure S1).

Compounds with substituents at the 3-position (**24**, **25**), including carboxamide substituents, **30**, **31**, and **39**, demonstrated a small increase in activity over **8TQ**. With this

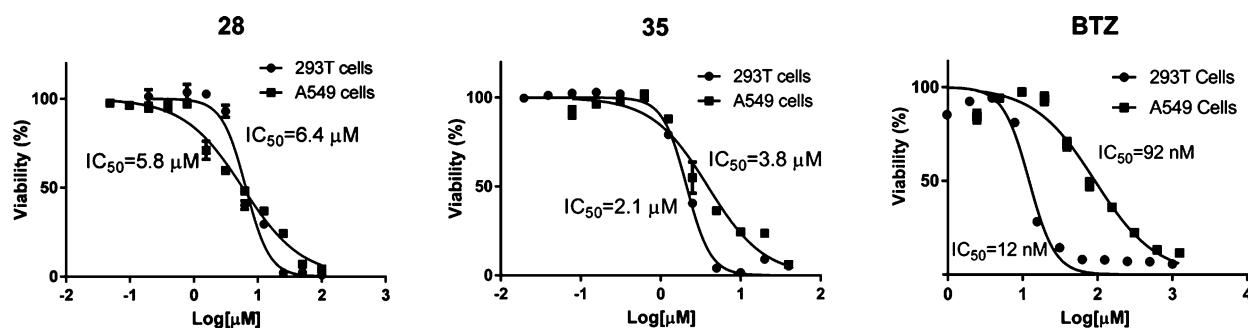
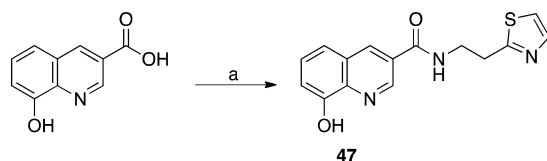


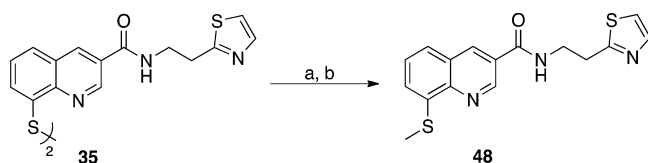
Figure 4. Cytotoxicity assay against 293T and A549 cancer cell lines with compounds 28 and 35; bortezomib (BTZ) was also included as an internal control.

Scheme 9. Synthesis of an 8-Hydroxyquinoline MBP-Based Analogue^a



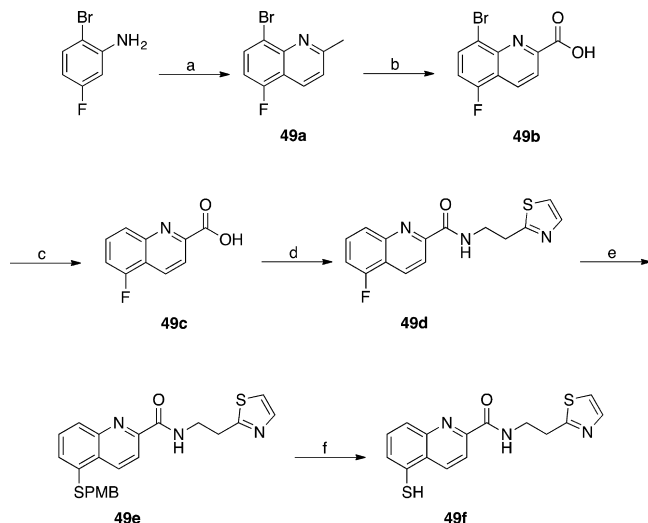
^a2-(Thiazol-2-yl)ethan-1-amine, HATU, Et₃N, DMF, 25 °C.

Scheme 10. Synthesis of a Methylated Analogue of Lead Compound 35^a



^aNaBH₄, MeOH, 25 °C; (b) CH₃I, THF, reflux.

Scheme 11. Synthesis of Compound 49f, a Structural-Isomer Analogue of Lead Compound 35^a



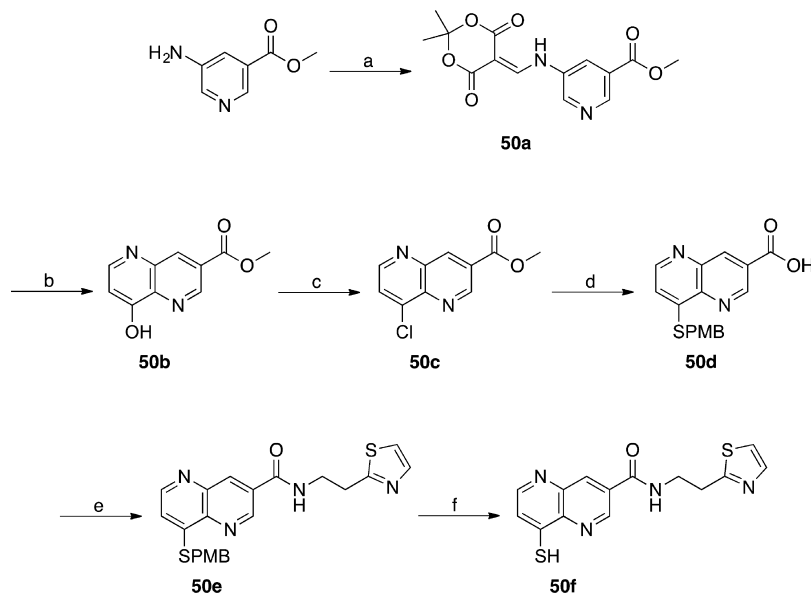
^aCrotonaldehyde, toluene, 6 M HCl, reflux; (b) SeO₂, pyridine, reflux; (c) Pd(OH)₂/C, 1 M NaOH, MeOH, H₂, 25 °C; (d) 2-(thiazol-2-yl)ethan-1-amine, HATU, Et₃N, DMF, 25 °C; (e) *p*-MBSH, NaH, DMF, 140 °C; (f) *m*-cresol, TFA, reflux.

preliminary SAR, a variety of substituents were explored via an amide linkage as illustrated in Table 3. The introduction of 5-

or 6-membered heterocyclic, aromatic rings, such as thiophene, thiazole, furan, oxazole, and pyridine (27–37), improved activity. In addition, compounds 27–37 all demonstrated better solubility in aqueous solution (data not shown). A trend was observed wherein the heterocycles containing a thiophene ring (31 and 34) demonstrated better activity than furan-based analogues (30 and 33). Introduction of thiazole heterocycles demonstrated similar inhibition to thiophene containing compounds; however, thiazole-containing compounds (28, 32, and 35) all demonstrated improved selectivity for Rpn11 over Csn5 and AMSH. The introduction of a phenyl (39) or functionalized phenyl (40–44) aromatic groups also improved the activity of the compounds; however, solubility in aqueous solution was poor (data not shown). Compounds 40 and 42 showed the best activity against Rpn11 (IC₅₀ value <200 nM, Table 3); however, the phenyl substituted compounds demonstrated poor selectivity over AMSH and also failed to show any cell-based activity. A pair of saturated ring derivatives was also explored (29 and 45), but these compounds consistently demonstrated poor activity. From this series of aryl substituted compounds (24–45), compound 35 showed the best overall characteristics and performance. Compound 35 showed submicromolar activity in the Rpn11 biochemical assay (IC₅₀ value 0.39 ± 0.04 μM) and ~100-fold selectivity over Csn5 and ~10-fold selectivity over AMSH. Compound 35 also demonstrated cytotoxicity toward 293T and A549 cells with an IC₅₀ of 2.1 and 3.8 μM, respectively. Lastly, a series of 35 MBP analogues further validated the SAR and mode of inhibition. Compound 47 utilizes a harder Lewis base 8-hydroxyquinoline MBP that displays poor activity against Rpn11. This suggests that the soft Lewis base character of the 8-thioquinoline results in better affinity for the active site Zn²⁺ ion. Evaluation of 48 and 49f revalidates the necessity of placing the coordinating atoms at the 1- and 8- positions. Finally, compound 50f uses fragment 8e (Scheme 3) instead of 8TQ as the MBP. Compound 50f showed activity against Rpn11 (~82 μM) but was significantly less active when compared to 35 (0.39 μM). This is consistent with the activity of the core scaffolds, fragments 8TQ and 8e, where 8TQ shows better activity against Rpn11 than 8e, again wholly consistent with metal coordination and formation of a 35-Rpn11 ternary complex as the mechanism of action of these inhibitors.

CONCLUSIONS

Proteasome inhibitors represent an expanding area with a broad therapeutic potential; however, limitations with current FDA approved inhibitors have generated interest in developing novel compounds. By utilizing a FBDD approach, a first-in-class,

Scheme 12. Synthesis of Compound 50f, an MBP Analogue of Lead Compound 35^a

^aMeldrum's acid, triethylformate, 100 °C; (b) Dowtherm A, 250 °C; (c) POCl₃, toluene, 110 °C; (d) *p*-MBSH, NaH, DMF, 25 °C; (e) 2-(thiazol-2-yl)ethan-1-amine, pyridine, EDC, HOBT, DMF, 25 °C; (f) *m*-cresol, TFA, reflux.

Table 5. Inhibitory Activity against Rpn11, Csn5, and AMSH for Control Compounds^a

compd	Rpn11 IC ₅₀ (μM)	Csn5 IC ₅₀ (μM)	AMSH IC ₅₀ (μM)	Ub ^{G76} V ^{GFP} HeLa Cell IC ₅₀ (μM)
47	>40	>100	>100	>100
48	>40	>100	>100	>100
49f	>100	35 ± 9	>100	>100
50f	82 ± 14	>100	>100	>100

^aCellular levels of proteasome inhibition are also listed.

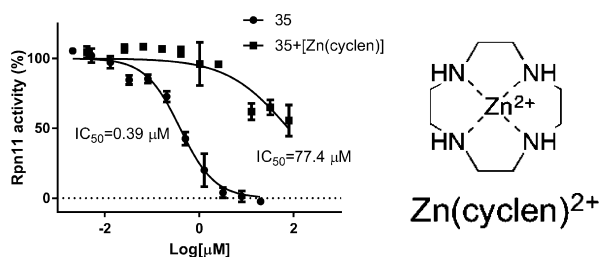


Figure 5. Inhibition of 35 against Rpn11 in the presence of Zn(cyclen)²⁺. Inhibition of 35 was also measured in the absence of Zn(cyclen)²⁺.

Rpn11-selective inhibitor with submicromolar IC₅₀ values that is cytotoxic toward cancer cell lines has been obtained. By utilizing a modest library of <100 fragments, we identified a fragment with low micromolar IC₅₀ values for Rpn11. The power of this approach was underscored by a high-throughput screen of >300000 compounds, which yielded a thioester derivative of 8TQ as the only hit that satisfied all criteria.²⁵ A series of compounds helped establish rudimentary SAR, and from this an inhibitor that blocks proliferation of cancer cells was obtained. Further biological characterization of the lead compound, 35, are described elsewhere.²⁵ Through inhibition of Rpn11 the ubiquitin tagged to the protein destined for degradation cannot be removed, thereby causing the proteasome to become inhibited. This represents a completely

new mode of action for a proteasome inhibitor and thus has potential for novel applications in the chemotherapy of cancer.

EXPERIMENTAL SECTION

General Experimental Details. All reagents and solvents were obtained from commercial sources and used without further purification. Microwave reactions were performed in 10 or 35 mL microwave vials using a CEM Discover S reactor. Column chromatography was performed using a Teledyne ISCO CombiFlash Rf system with prepacked silica cartridges or High Performance Gold C18 columns. ¹H/¹³C NMR spectra were recorded at ambient temperature on a 400 or 500 Varian FT-NMR instrument located in the Department of Chemistry and Biochemistry at the University of California, San Diego. Mass spectra were obtained at the Molecular Mass Spectrometry Facility (MMSF) in the Department of Chemistry and Biochemistry at the University of California, San Diego. The purity of all compounds used in assays was determined to be ≥95% by ¹H NMR spectroscopy and confirmed by high-resolution mass spectrometry (HRMS) and liquid chromatography–mass spectrometry (LC-MS) analysis using an Agilent 6230 Accurate-Mass LC-TOFMS at the MMSF (University of California, San Diego).

Synthetic Procedures and Compound Characterization. 8-(Methylthio)quinoline (6). To a solution of 8-thioquinoline (0.07 g, 0.35 mmol) in a mixture of EtOH, H₂O, and 2 M NaOH (4 mL, 2:1:1 ratio) was added CH₃I (0.120 mL, 1.8 mmol). The solution was stirred at room temperature for 24 h and then evaporated to dryness. The reaction mixture was then dissolved in CH₂Cl₂ and washed with H₂O (3 × 50 mL). The combined organic layers were dried and concentrated in vacuo. The crude was purified via silica gel column chromatography eluting a gradient of 0–100% EtOAc in hexanes. Yield = 0.006 g (10%). ¹H NMR (500 MHz, CDCl₃): δ 8.95 (dd, *J* = 4.2, 1.8 Hz, 1H), 8.14 (dd, *J* = 8.3, 1.7 Hz, 1H), 7.57 (dd, *J* = 8.2, 1.3 Hz, 1H), 7.50 (dd, *J* = 8.1, 7.3 Hz, 1H), 7.45 (dd, *J* = 8.2, 4.2 Hz, 1H), 7.41 (dd, *J* = 7.4, 1.3 Hz, 1H), 2.59 (s, 3H). ESI-MS (+): *m/z* 176.11 [*M* + H]⁺.

5-Chloroquinoline (7a). A solution of 5-hydroxyquinoline (0.1 g, 0.68 mmol) in POCl₃ (5 mL) was stirred at 100 °C for 2 h. H₂O was added slowly to the reaction mixture to neutralize POCl₃, and the resulting solution was evaporated to dryness. To the resulting crude was added MeOH, which caused the formation of a white precipitate. The solid was isolated by filtration to afford product. Yield = 0.08 g

(71%). ^1H NMR (400 MHz, DMSO- d_6): δ 8.93–8.89 (m, 1H), 8.47 (t, J = 6.8 Hz, 1H), 7.78 (d, J = 5.5 Hz, 1H), 7.74–7.67 (m, 1H), 7.60–7.54 (m, 1H), 7.46 (d, J = 6.6 Hz, 1H). ESI-MS (+): m/z 164.05 $[\text{M} + \text{H}]^+$.

5-(tert-Butylthio)quinolone (7b). To a solution of **7a** (0.07 g, 0.43 mmol) in DMF (7 mL) was added NaH (0.035 g, 1.45 mmol) and *tert*-butylthiol (*t*-BuSH, 0.97 mL, 0.86 mmol) under nitrogen atmosphere. The reaction was stirred at 140 °C for 18 h. The resulting solution was then concentrated in vacuo, and the crude material was purified via silica gel column chromatography eluting a gradient of 0–100% EtOAc in hexanes. Yield = 0.04 g (43%). ^1H NMR (400 MHz, CD_3OD): δ 8.89 (dd, J = 4.3, 1.8 Hz, 1H), 8.58–8.53 (m, 1H), 7.68 (d, J = 8.4 Hz, 1H), 7.55–7.46 (m, 1H), 7.38 (dd, J = 8.4, 4.3 Hz, 1H), 6.85 (d, J = 7.7 Hz, 1H), 1.53 (s, 9H). ESI-MS (+): m/z 218.15 $[\text{M} + \text{H}]^+$.

Quinoline-5-thiol (7c). A solution of **7b** (0.04 g, 0.17 mmol) in conc HCl (11 mL) was stirred at 100 °C for 19 h. The resulting solution was neutralized to pH 9–10 with NaOH and extracted twice with CHCl_3 (3×10 mL). The combined organic layers were dried, and the solution was concentrated in vacuo. The crude material was then recrystallized from EtOAc. Yield = 0.01 g (48%). ^1H NMR (500 MHz, CDCl_3): δ 8.95–8.90 (m, 1H), 8.66–8.56 (m, 1H), 7.75–7.70 (m, 1H), 7.60–7.50 (m, 1H), 7.45–7.36 (m, 1H), 6.93–6.85 (m, 1H). ESI-MS (+): m/z 162.10 $[\text{M} + \text{H}]^+$.

2,2-Dimethyl-5-(pyridin-3-ylamino)methylene)-1,3-dioxane-4,6-dione (8a). To a preheated (~ 100 °C) mixture of 3-aminopyridine (0.37 g, 4.0 mmol) and 2,2-dimethyl-[1,3]dioxane-4,6-dione (Meldrum's acid, 0.69 g, 4.8 mmol) was added triethyl orthoformate (4.0 mL, 24.0 mmol). The solution was stirred at 100 °C for 2 h. The reaction proceeded by changing color from yellow to wine-red accompanying the formation of a yellow precipitate. After cooling to room temperature, the excess liquid of triethyl orthoformate was removed via vacuum distillation. The resulting solid was purified via silica gel chromatography eluting a gradient of 70–100% EtOAc in hexanes. Yield = 0.72 g (72%). ^1H NMR (400 MHz, CDCl_3): δ 11.25 (d, J = 10.4 Hz, 1H), 8.63 (d, J = 14.00 Hz, 1H), 8.61 (d, J = 3.2 Hz, 1H), 8.55 (dd, J = 4.8 Hz, J = 1.6 Hz, 1H), 7.61 (d, J = 8.0 Hz, 1H), 7.41 (dd, J = 8.20, 4.2 Hz, 1H), 1.77 (s, 6H). ^{13}C NMR (100 MHz, CDCl_3): δ 165.2, 163.0, 152.9, 147.6, 140.6, 134.6, 124.9, 124.1, 105.2, 88.5, 26.9. ESI-MS (+): m/z 248.90 $[\text{M} + \text{H}]^+$.

1,5-Naphthyridin-4-ol (8b). To a flask containing **8a** (2.6 g, 10.4 mmol) under nitrogen atmosphere was added Dowtherm A (150 mL) and placed in a preheated oil bath at 250 °C. The reaction mixture was stirred at reflux for 1 h. A color change from orange–yellow to dark-brown was observed. The resulting solution was cooled to room temperature and filtered to isolate solid product. The solid was rinsed with diphenyl ether and acetone to give the desired product as a dark solid. Yield = 1.14 g (75%). ^1H NMR (400 MHz, CD_3OD + one drop TFA): δ 9.07 (d, J = 4.8 Hz, 1H), 8.72 (d, J = 8.8 Hz, 1H), 8.61 (d, J = 7.2 Hz, 1H), 8.22 (dd, J = 8.8 Hz, J = 4.8 Hz, 1H), 7.07 (d, J = 7.2 Hz, 1H). ^{13}C NMR (125 MHz, CD_3OD + one drop TFA): δ 172.3, 147.5, 145.5, 138.6, 134.8, 134.4, 130.1, 112.2. ESI-MS (+): m/z 147.29 $[\text{M} + \text{H}]^+$.

4-Chloro-1,5-naphthyridine (8c). To a solution of **8b** (0.8 g, 5.47 mmol) in toluene (20 mL) was added POCl_3 (1.02 mL, 10.95 mmol) at room temperature. The solution was stirred at 110 °C for 2 h, then allowed to cool to room temperature, resulting in the formation of a precipitate. The solution and dark solid was quenched with saturated NaHCO_3 (aq) and extracted with EtOAc. The combined organic layers were dried over anhydrous Na_2SO_4 , filtered, and concentrated under reduced pressure. The residue was purified via silica gel chromatography eluting a gradient of 20–40% EtOAc in CH_2Cl_2 . Yield = 0.37 g (41%). ^1H NMR (400 MHz, CDCl_3): δ 8.92 (dd, J = 4.4, 1.2 Hz, 1H), 8.69 (d, J = 4.8 Hz, 1H), 8.26 (dd, J = 8.8, 1.6 Hz, 1H), 7.60 (d, J = 8.0 Hz, 1H), 7.56 (dd, J = 8.4, 4.0 Hz, 1H). ^{13}C NMR (100 MHz, CDCl_3): δ 151.4, 151.3, 150.5, 144.7, 143.9, 140.7, 137.8, 125.2, 124.3. ESI-MS (+): m/z 165.28 $[\text{M} + \text{H}]^+$.

4-(4-Methoxybenzyl)thio)-1,5-naphthyridine (8d). To a solution of **8c** (0.9 g, 5.47 mmol) in DMF (30 mL) was added (4-methoxyphenyl)methanethiol (*p*-MBSH, 1.1 mL, 8.20 mmol) and

NaH (0.49 g, 16.4 mmol, 60 wt %) at room temperature. The solution was stirred for 2 h, then quenched with MeOH and concentrated in vacuo. The resulting residue was diluted with H_2O and neutralized with 1 N HCl to pH \sim 8. The aqueous solution was extracted with EtOAc. The combined organic layers were dried over anhydrous Na_2SO_4 , filtered, and concentrated under reduced pressure. The crude material was purified via silica gel chromatography eluting a gradient of 25–70% EtOAc in hexanes. Yield = 1.07 g (70%). ^1H NMR (400 MHz, CDCl_3): δ 8.90 (dd, J = 4.4, 1.6 Hz, 1H), 8.69 (d, J = 4.8 Hz, 1H), 8.33 (dd, J = 8.4, 1.6 Hz, 1H), 7.63 (dd, J = 8.4, 4.8 Hz, 1H), 7.39 (d, J = 9.2 Hz, 2H), 7.35 (d, J = 4.8 Hz, 1H), 6.86 (dd, J = 8.8 Hz, 2H), 4.24 (s, 2H), 3.77 (s, 3H). ^{13}C NMR (125 MHz, CDCl_3): δ 159.2, 151.4, 150.1, 149.5, 142.6, 141.7, 137.7, 130.1, 130.1, 126.9, 125.0, 118.1, 114.3, 55.4, 34.8. ESI-MS (+): m/z 283.05 $[\text{M} + \text{H}]^+$.

1,5-Naphthyridine-4-thiol (8e). To a solution of **8d** (0.7 g, 2.48 mmol) in TFA (20 mL) was added *m*-cresol (1.3 mL, 12.41 mmol) at room temperature. The solution was then stirred at reflux for 16 h and then allowed to cool. The resulting reaction mixture was concentrated and diluted with the EtOAc. The solution was neutralized with saturated NaHCO_3 (aq), which resulted in the formation of an orange–red precipitate. The precipitate was collected via vacuum filtration and washed with H_2O and acetone to yield the desired product. Yield = 0.38 g (94%). ^1H NMR (400 MHz, CDCl_3): δ 8.70–8.63 (m, 1H), 8.03 (dd, J = 7.8, 2.2 Hz, 1H), 7.95 (d, J = 4.8 Hz, 1H), 7.46 (dd, J = 8.2, 4.2 Hz, 1H), 7.41 (d, J = 5.2 Hz, 1H). ^{13}C NMR (100 MHz, CDCl_3): δ 174.2, 148.4, 147.2, 146.7, 143.4, 137.42, 128.2, 122.8. ESI-MS (+): m/z 163.19 $[\text{M} + \text{H}]^+$.

8-Fluoro-2-methylquinoline (9a). To a solution of 2-fluoroaniline (1 g, 9 mmol) in toluene (40 mL) was added 6 M HCl (12 mL) and crotonaldehyde (1.47 mL, 1.8 mmol). The heterogeneous mixture was stirred at 110 °C for 2 h. The aqueous layer was separated, neutralized to pH 9, and extracted with EtOAc (3×50 mL). The combined organic layers were dried over anhydrous MgSO_4 , filtered, and concentrated under reduced pressure. The crude material was purified via silica gel column chromatography eluting a gradient of 0–100% EtOAc in hexanes. Yield = 0.71 g (49%). ^1H NMR (400 MHz, DMSO- d_6): δ 8.29 (d, J = 9.5 Hz, 1H), 7.71 (d, J = 7.0 Hz, 1H), 7.56–7.40 (m, 3H), 2.66 (s, 3H). ESI-MS (+): m/z 162.2 $[\text{M} + \text{H}]^+$.

8-(tert-Butylthio)-2-methylquinoline (9b). To a solution of **9a** (0.195 g, 1.21 mmol) in DMF (20 mL) was added NaH (0.097 g, 4.04 mmol) and *t*-BuSH (0.272 mL, 2.42 mmol) under nitrogen atmosphere. The solution was stirred at 140 °C for 18 h. The reaction mixture was evaporated to dryness, and the crude material was purified via silica gel column chromatography eluting a gradient of 0–100% EtOAc in hexanes. Yield = 0.22 g (77%). ^1H NMR (400 MHz, CDCl_3): δ 8.74 (d, J = 8.3 Hz, 1H), 8.27 (dd, J = 7.2, 1.3 Hz, 1H), 8.17–8.04 (m, 1H), 7.81 (t, J = 7.8 Hz, 1H), 7.75 (d, J = 8.4 Hz, 1H), 3.59 (s, 3H), 1.43 (s, 9H). ESI-MS (+): m/z 231.91 $[\text{M} + \text{H}]^+$.

2-Methylquinoline-8-thiol (9c). A solution of **9b** (0.04 g, 0.17 mmol) in conc HCl (11 mL) was stirred at 100 °C for 19 h. The solution was neutralized to pH 9–10 and extracted EtOAc (3×10 mL). The combined organic layers were dried over anhydrous MgSO_4 , filtered, and concentrated under reduced pressure. The crude material was recrystallized from EtOH. Yield = 0.02 g (66%). ^1H NMR (500 MHz, CDCl_3): δ 8.07 (d, J = 8.4 Hz, 1H), 7.85 (d, J = 7.5 Hz, 1H), 7.58 (d, J = 8.0 Hz, 1H), 7.41–7.30 (m, 2H), 2.85 (s, 3H). APCI-MS (–): m/z 174.10 $[\text{M} - \text{H}]^-$.

8-Fluoro-3-methylquinoline (10a). To a solution of 2-fluoroaniline (1.0 g, 9 mmol) in toluene (40 mL) was added 6 M HCl (12 mL) and methacrolein (1.5 mL, 1.8 mmol). The heterogeneous mixture was stirred at 110 °C for 2.5 h. The aqueous layer was separated, neutralized to pH 9, and extracted with EtOAc (3×50 mL). The combined organic layers were dried over anhydrous MgSO_4 , filtered, and concentrated under reduced pressure. The crude material was purified via silica gel column chromatography eluting a gradient of 0–100% EtOAc in hexanes. Yield = 0.65 g (45%). ^1H NMR (500 MHz, CDCl_3): δ 8.53 (d, J = 2.3 Hz, 1H), 7.56 (s, 1H), 7.22–7.17 (m, 1H), 7.17–7.10 (m, 1H), 7.08–6.98 (m, 1H), 2.22–2.21 (s, 3H). ESI-MS (+): m/z 162.19 $[\text{M} + \text{H}]^+$.

8-(tert-Butylthio)-3-methylquinoline (10b). To a solution of **10a** (0.5 g, 3.1 mmol) in DMF (50 mL) was added NaH (0.25 g, 10.3 mmol) and *t*-BuSH (0.698 mL, 6.2 mmol) under nitrogen atmosphere. The reaction mixture was stirred at 140 °C for 18 h. The resulting solution was evaporated to dryness and the crude material purified via silica gel column chromatography eluting a gradient of 0–100% EtOAc in hexanes. Yield = 0.56 g (78%). ¹H NMR (500 MHz, CDCl₃): δ 8.90 (d, *J* = 2.3 Hz, 1H), 7.96 (dd, *J* = 7.2, 1.5 Hz, 1H), 7.92 (d, *J* = 1.1 Hz, 1H), 7.74 (dd, *J* = 8.2, 1.5 Hz, 1H), 7.47 (dd, *J* = 8.1, 7.2 Hz, 1H), 2.53 (s, 3H), 1.37 (s, 9H). ESI-MS(+): *m/z* 231.92 [M + H]⁺.

3-Methylquinoline-8-thiol (10c). A solution of **10b** (0.08 g, 0.35 mmol) in conc HCl (25 mL) was stirred at 100 °C for 19 h. The reaction mixture was neutralized to pH 9 with NaOH and extracted with EtOAc (3 × 10 mL). The combined organic layers were dried over anhydrous MgSO₄, filtered, and concentrated under reduced pressure. The crude material was purified via silica gel column chromatography eluting a gradient of 0–100% EtOAc in hexanes. Yield = 0.02 g (33%). ¹H NMR (500 MHz, CDCl₃): δ 8.73 (d, *J* = 8.4 Hz, 1H), 7.85 (d, *J* = 7.5 Hz, 1H), 7.60 (d, *J* = 8.0 Hz, 1H), 7.47–7.45 (m, 1H), 7.35–7.31 (m, 1H), 5.58 (s, 1H), 2.48 (s, 3H). ESI-MS(+): *m/z* 176.16 [M + H]⁺.

8-Fluoro-4-methylquinoline (11a). To a solution of 2-fluoroaniline (1.0 g, 9 mmol) in toluene (40 mL) was added 6 M HCl (12 mL) and methyl vinyl ketone (1.5 mL, 1.8 mmol). The heterogeneous mixture was stirred at 110 °C for 16 h. The aqueous layer was separated, neutralized to pH 9 with 6 M NaOH, and extracted with CH₂Cl₂ (3 × 50 mL). The combined organic layers were dried over anhydrous MgSO₄, filtered, and concentrated under reduced pressure. The crude material was purified via silica gel column chromatography eluting a gradient of 0–100% EtOAc in hexanes. Yield = 0.4 g (28%). ¹H NMR (500 MHz, DMSO-*d*₆): δ 8.74 (d, *J* = 4.4 Hz, 1H), 7.83–7.77 (m, 1H), 7.57–7.46 (m, 2H), 7.39 (dd, *J* = 4.3, 1.0 Hz, 1H), 2.61 (s, 3H). ESI-MS(+): *m/z* 162.23 [M + H]⁺.

8-(tert-Butylthio)-4-methylquinoline (11b). To a solution of **11a** (0.26 g, 1.58 mmol) in DMF (25 mL) was added NaH (0.13 g, 5.29 mmol) and *t*-BuSH (0.356 mL, 3.16 mmol) under nitrogen atmosphere. The solution was stirred at 140 °C for 18 h. The reaction mixture was evaporated to dryness, and the crude material was purified via silica gel column chromatography eluting a gradient of 0–100% EtOAc in hexanes. Yield = 0.2 g (55%). ¹H NMR (500 MHz, CDCl₃): δ 8.88 (d, *J* = 4.3 Hz, 1H), 8.05–7.93 (m, 2H), 7.50 (dd, *J* = 8.4, 7.2 Hz, 1H), 7.22 (dd, *J* = 4.3, 1.0 Hz, 1H), 2.69 (s, 3H), 1.36 (s, 9H). ESI-MS(+): *m/z* 231.90 [M + H]⁺.

4-Methylquinoline-8-thiol (11c). A solution of **11b** (0.08 g, 0.35 mmol) in conc HCl (25 mL) was stirred at 100 °C for 19 h. The reaction mixture was neutralized to pH 9 with NaOH and extracted with EtOAc (3 × 50 mL). The combined organic layers were dried over anhydrous MgSO₄, filtered, and concentrated under reduced pressure. The crude material was purified via silica gel column chromatography eluting a gradient of 0–100% EtOAc in hexanes. Yield = 0.02 g (30%). ¹H NMR (500 MHz, CDCl₃): δ 8.76 (d, *J* = 4.4 Hz, 1H), 7.76–7.66 (m, 2H), 7.39 (dd, *J* = 8.4, 7.3 Hz, 1H), 7.25 (dd, *J* = 4.4, 1.0 Hz, 1H), 2.69 (s, 3H). ESI-MS(+): *m/z* 176.17 [M + H]⁺.

8-Chloro-5-methylquinoline (12a). To a solution of 2-chloro-5-methylaniline (1 g, 14.1 mmol) in 75% sulfuric acid (8 mL) was added nitrobenzene (1.44 mL, 14.1 mmol) and glycerol (2.06 mL, 28.2 mmol). The heterogeneous mixture was stirred at 150 °C for 2 h. This was allowed to cool, then H₂O was added to the mixture and extracted with EtOAc (3 × 50 mL). The combined organic layers were dried over anhydrous MgSO₄, filtered, and concentrated under reduced pressure. The crude material was purified via silica gel column chromatography, eluting a gradient of 0–100% EtOAc in hexanes. Yield = 1.0 g (40%). ¹H NMR (500 MHz, CDCl₃): δ 9.04 (dd, *J* = 4.2, 1.7 Hz, 1H), 8.32 (dd, *J* = 8.5, 1.7 Hz, 1H), 7.71 (d, *J* = 7.7 Hz, 1H), 7.49 (dd, *J* = 8.5, 4.2 Hz, 1H), 7.28 (dd, *J* = 7.8, 0.9 Hz, 1H), 2.65 (d, *J* = 1.0 Hz, 3H). ESI-MS(+): *m/z* 178.21 [M + H]⁺.

8-(tert-Butylthio)-5-methylquinoline (12b). To a solution of **12a** (1 g, 5.62 mmol) in DMF (100 mL) was added NaH (0.45 g, 18.8 mmol) and *t*-BuSH (1.26 mL, 3.16 mmol) under nitrogen atmosphere.

The reaction mixture was stirred at 140 °C for 18 h. The resulting solution was evaporated to dryness, and the crude material purified via silica gel column chromatography, eluting a gradient of 0–100% EtOAc in hexanes. Yield = 0.19 g (14%). ¹H NMR (500 MHz, CDCl₃): δ 9.05 (dd, *J* = 4.2, 1.7 Hz, 1H), 8.34 (dd, *J* = 8.5, 1.7 Hz, 1H), 7.72 (d, *J* = 7.6 Hz, 1H), 7.50 (dd, *J* = 8.5, 4.2 Hz, 1H), 7.29 (dd, *J* = 7.6, 1.0 Hz, 1H), 2.66 (d, *J* = 1.0 Hz, 3H), 1.34 (s, 9H). ESI-MS(+): *m/z* 231.91 [M + H]⁺.

5-Methylquinoline-8-thiol (12c). A solution of **12b** (0.08 g, 0.35 mmol) in conc HCl (25 mL) was stirred at 100 °C for 19 h. The resulting solution was neutralized to pH 9 with NaOH and extracted with EtOAc (3 × 50 mL). The combined organic layers were dried and concentrated under reduced pressure. The crude material was purified via silica gel column chromatography eluting a gradient of 0–100% EtOAc in hexanes. Yield = 0.05 g (81%). ¹H NMR (500 MHz, CDCl₃): δ 8.94 (dd, *J* = 4.3, 1.8 Hz, 1H), 8.09 (dd, *J* = 8.3, 1.8 Hz, 1H), 7.79 (d, *J* = 1.8 Hz, 1H), 7.45 (dd, *J* = 8.3, 4.3 Hz, 1H), 7.38 (s, 1H), 2.39 (s, 3H). ESI-MS(+): *m/z* 176.00 [M + H]⁺.

8-Fluoro-6-methylquinoline (13a). To a solution of 2-fluoro-6-methylaniline (0.5 g, 4.0 mmol) in 75% sulfuric acid (4 mL) was added nitrobenzene (0.409 mL, 4.0 mmol) and glycerol (0.588 mL, 8.0 mmol). The heterogeneous mixture was stirred at 150 °C for 3 h, then allowed to cool to room temperature. H₂O was added to the reaction mixture and with EtOAc (3 × 50 mL). The combined organic layers were dried over anhydrous MgSO₄, filtered, and concentrated under reduced pressure. The crude material was purified via silica gel column chromatography eluting a gradient of 0–100% EtOAc in hexanes. Yield = 0.17 g (27%). ¹H NMR (500 MHz, CDCl₃): δ 8.79 (dd, *J* = 4.2, 1.6 Hz, 1H), 7.99 (d, *J* = 8.4 Hz, 1H), 7.92 (s, 1H), 7.34 (dd, *J* = 8.4, 4.2 Hz, 1H), 7.15 (dd, *J* = 11.5, 1.8 Hz, 1H), 2.43 (d, *J* = 1.0 Hz, 3H). ESI-MS(+): *m/z* 162.19 [M + H]⁺.

8-(tert-Butylthio)-6-methylquinoline (13b). To a solution of **13a** (0.14 g, 0.87 mmol) in DMF (14 mL) was added NaH (0.07 g, 2.91 mmol) and *t*-BuSH (0.196 mL, 1.74 mmol) under nitrogen atmosphere. The solution was stirred at 140 °C for 18 h. The resulting solution was evaporated to dryness and the crude material purified via silica gel column chromatography using a gradient of 0–100% EtOAc in hexanes. Yield = 0.16 g (78% yield). ¹H NMR (500 MHz, CDCl₃): δ 8.98 (dd, *J* = 4.2, 1.8 Hz, 1H), 8.06 (dd, *J* = 8.2, 1.8 Hz, 1H), 7.89 (d, *J* = 2.0 Hz, 1H), 7.58 (d, *J* = 1.0 Hz, 1H), 7.37 (dd, *J* = 8.2, 4.2 Hz, 1H), 2.54 (s, 3H), 1.37 (s, 9H). ESI-MS(+): *m/z* 231.91 [M + H]⁺.

6-Methylquinoline-8-thiol (13c). A solution of **13b** (0.08 g, 0.35 mmol) in conc HCl (25 mL) was stirred at 100 °C for 19 h. The crude material was neutralized to pH 9 with NaOH and extracted with EtOAc (3 × 50 mL). The combined organic layers were dried over anhydrous MgSO₄, filtered, and concentrated under reduced pressure. The crude material was purified via silica gel column chromatography eluting a gradient of 0–100% EtOAc in hexanes. Yield = 0.03 g (46%). ¹H NMR (400 MHz, CDCl₃): δ 8.84 (dd, *J* = 4.3, 1.6 Hz, 1H), 8.03 (dd, *J* = 8.2, 1.6 Hz, 1H), 7.55 (d, *J* = 1.8 Hz, 1H), 7.38 (dd, *J* = 8.2, 4.2 Hz, 1H), 7.31 (d, *J* = 0.9 Hz, 1H), 5.61 (s, 1H), 2.46 (s, 3H). ESI-MS(+): *m/z* 176.17 [M + H]⁺.

8-(tert-Butylthio)quinoline-2-carboxylic Acid (14a). To a solution of 8-fluoroquinoline-2-carboxylic acid (0.42 g, 2.19 mmol) in DMF (40 mL) was added NaH (0.18 g, 7.29 mmol) and *t*-BuSH (0.495 mL, 4.4 mmol) under nitrogen atmosphere. The solution was stirred at 140 °C for 18 h. The reaction mixture was evaporated to dryness and the crude material was taken in H₂O and acidified with 1 M HCl until a precipitate was formed (pH 2). The precipitate was filtered and dried under vacuum. Yield = 0.45 g (78%). ¹H NMR (400 MHz, CDCl₃): δ 8.42 (dd, *J* = 8.5, 2.4 Hz, 1H), 8.32 (dd, *J* = 6.6, 3.7 Hz, 1H), 8.12 (d, *J* = 6.8 Hz, 1H), 7.94 (d, *J* = 7.2 Hz, 1H), 7.70–7.62 (m, 1H), 1.35–1.30 (m, 9H). ESI-MS(+): *m/z* 261.96 [M + H]⁺.

8,8'-Disulfanediylbis(quinoline-2-carboxylic Acid) (14b). A solution of **14a** (0.24 g, 0.92 mmol) in conc HCl (40 mL) was stirred at 110 °C for 12 h. The solution was neutralized to pH 9 and washed with EtOAc (3 × 50 mL). The aqueous layer was then acidified to pH 2–3, and the precipitate was collected via vacuum filtration. The product was isolated as a disulfide dimer as evidenced by mass

spectrometry. Yield = 0.15 g (80%). ^1H NMR (400 MHz, $\text{DMSO}-d_6$): δ 8.61 (d, J = 8.5 Hz, 1H), 8.21 (d, J = 8.6 Hz, 1H), 7.92 (d, J = 8.0 Hz, 1H), 7.83 (d, J = 7.3 Hz, 1H), 7.63 (t, J = 7.8 Hz, 1H). ESI-MS (–): m/z 407.05 $[\text{M} - \text{H}]^-$.

Dimethyl 8,8'-Disulfanediylbis(quinoline-2-carboxylate) (15). In a 10 mL microwave tube was placed **14b** (0.02 g, 0.97 mmol) and MeOH (2 mL), followed by 15 drops of conc H_2SO_4 . The solution was placed in a microwave reactor and heated to 90 °C with stirring for 24 min. The solution was evaporated to dryness, and the crude material was taken up in CHCl_3 and washed with a satd NaHCO_3 (3 \times 50 mL). The combined organic layers were dried over anhydrous MgSO_4 , filtered, and concentrated under reduced pressure. Yield = 0.02 g (84%). ^1H NMR (400 MHz, CDCl_3): δ 8.33 (dd, J = 8.7, 1.4 Hz, 1H), 8.26 (dd, J = 8.5, 1.4 Hz, 1H), 7.95 (d, J = 7.5 Hz, 1H), 7.68 (d, J = 8.2 Hz, 1H), 7.47 (td, J = 7.8, 1.5 Hz, 1H), 4.10 (s, 3H). ESI-MS(+): m/z 437.16 $[\text{M} + \text{H}]^+$.

8-(tert-Butylthio)quinoline-3-carboxylic Acid (16a). To a solution of 8-fluoroquinoline-3-carboxylic acid (1 g, 5.2 mmol) in DMF (40 mL) was added NaH (0.5 g, 20.8 mmol) and *t*-BuSH (2.35 mL, 20.8 mmol) under nitrogen atmosphere. The reaction mixture was stirred at 140 °C for 18 h. The solution was evaporated to dryness, and the crude material was taken up in H_2O and acidified with 6 M HCl until a precipitate was formed (pH 2). The precipitate was filtered and dried under vacuum. Yield = 1.47 g (100%). ^1H NMR (400 MHz, $\text{DMSO}-d_6$): δ 9.35 (d, J = 2.0 Hz, 1H), 8.96 (d, J = 1.9 Hz, 1H), 8.20–8.15 (m, 1H), 8.10 (d, J = 7.2 Hz, 1H), 7.67 (dd, J = 8.2, 7.2 Hz, 1H), 1.30 (s, 9H). ESI-MS(+): m/z 261.97 $[\text{M} + \text{H}]^+$.

8,8'-Disulfanediylbis(quinoline-3-carboxylic Acid) (16b). A solution of **16a** (0.6 g, 2.3 mmol) in conc HCl (50 mL) was stirred at 100 °C for 12 h. The reaction mixture was neutralized to pH 9 and washed with EtOAc (3 \times 50 mL). The aqueous layer was then acidified to pH 2–3 and the observed precipitate collected via vacuum filtration. The crude material was recrystallized from EtOH. The product was isolated as a disulfide dimer as evidenced by mass spectrometry. Yield = 0.18 g (38%). ^1H NMR (400 MHz, $\text{DMSO}-d_6$): δ 9.38 (d, J = 1.6 Hz, 1H), 9.02 (d, J = 1.6 Hz, 1H), 8.04 (d, J = 8.0 Hz, 1H), 7.87 (d, J = 8.0 Hz, 1H), 7.62 (t, J = 7.8 Hz, 1H). ESI-MS(+): m/z 409.01 $[\text{M} + \text{H}]^+$.

Dimethyl 8,8'-Disulfanediylbis(quinoline-3-carboxylate) (17). In a 10 mL microwave tube was placed **16b** (0.020 g, 0.97 mmol) and MeOH (2 mL) followed by 15 drops of conc H_2SO_4 . The solution was placed in a microwave reactor and heated to 90 °C with stirring for 20 min. The solution was evaporated to dryness, and the crude material was taken up in CHCl_3 and washed with a satd solution of NaHCO_3 (3 \times 50 mL). The combined organic layers were dried over anhydrous MgSO_4 , filtered, and concentrated under reduced pressure. The crude material was recrystallized from EtOH. Yield = 0.004 g (19%). ^1H NMR (400 MHz, $\text{DMSO}-d_6$): δ 9.41 (d, J = 2.0 Hz, 1H), 9.10 (d, J = 2.0 Hz, 1H), 8.08 (d, J = 8.1 Hz, 1H), 7.89 (d, J = 7.5 Hz, 1H), 7.69–7.59 (m, 1H), 3.98 (s, 3H). ESI-MS(+): m/z 437.11 $[\text{M} + \text{H}]^+$.

8-Fluoroquinoline-4-carboxylic Acid (18b). To a solution of 7-fluoroisatin (0.5 g, 3.03 mmol) in H_2O (10 mL) in a 35 mL microwave tube was added 5 M NaOH (2.52 mL, 15.1 mmol) and sodium pyruvate (0.4 g, 3.66 mmol). The mixture was placed in a microwave reactor and heated to 110 °C with stirring for 10 min. After cooling to room temperature, the suspension containing the dicarboxylic acid derivative was acidified to pH 2 and the dark solid was filtered off to afford **18a**. A portion of **18a** (0.17 g) was then placed in a 10 mL microwave tube and H_2O (2 mL) was added. The resulting suspension was placed in a microwave reactor and heated to 170 °C (or 280 psi) with stirring for 5 min. The brown solid was collected via vacuum filtration. Yield = 60% over 2 steps. ^1H NMR (400 MHz, $\text{DMSO}-d_6$): δ 9.07 (d, J = 4.1 Hz, 1H), 8.48 (d, J = 7.4 Hz, 1H), 8.00 (d, J = 4.1 Hz, 1H), 7.73–7.62 (m, 2H). ESI-MS(+): m/z 192.27 $[\text{M} + \text{H}]^+$.

8-(tert-Butylthio)quinoline-4-carboxylic Acid (18c). To a solution of **18b** (0.3 g, 1.57 mmol) in DMF (30 mL) was added NaH (0.15 g, 6.3 mmol) and *t*-BuSH (0.707 mL, 36.3 mmol) under nitrogen atmosphere. The mixture was stirred at 140 °C for 18 h. The solution was evaporated to dryness and the crude material was taken up in H_2O and acidified with HCl until a precipitate formed (pH 2). The precipitate was collected via vacuum filtration and discarded. The

filtrate was extracted with EtOAc (3 \times 50 mL), dried over anhydrous MgSO_4 , filtered, and concentrated under reduced pressure. H_2O was then added to the crude material resulting in a yellow precipitate. The precipitate was collected by vacuum filtration. Yield = 0.2 g (49% yield). ^1H NMR (400 MHz, $\text{DMSO}-d_6$): δ 9.07 (d, J = 4.1 Hz, 1H), 8.60 (d, J = 8.6 Hz, 1H), 8.05 (d, J = 7.1 Hz, 1H), 7.90 (d, J = 4.3 Hz, 1H), 7.68 (t, J = 7.9 Hz, 1H), 1.30 (s, 9H). ESI-MS(+): m/z 261.93 $[\text{M} + \text{H}]^+$.

8,8'-Disulfanediylbis(quinoline-4-carboxylic Acid) (18d). A solution of **18c** (0.2 g, 0.76 mmol) in conc HCl (18 mL) was stirred at 100 °C for 12 h. The crude material was neutralized to pH 9 and washed EtOAc (3 \times 10 mL). The aqueous layer was then acidified to pH 2–3 with HCl, and the resulting precipitate was collected via vacuum filtration. The product was isolated as a disulfide dimer as evidenced by mass spectrometry. Yield = 0.09 g (58% yield). ^1H NMR (400 MHz, $\text{DMSO}-d_6$): δ 9.13 (d, J = 4.5 Hz, 1H), 8.49 (d, J = 8.5 Hz, 1H), 8.05 (d, J = 4.4 Hz, 1H), 7.78 (d, J = 7.5 Hz, 1H), 7.61 (t, J = 8.0 Hz, 1H). ESI-MS(–): m/z 406.96 $[\text{M} - \text{H}]^-$.

Dimethyl 8,8'-Disulfanediylbis(quinoline-4-carboxylate) (19). In a 10 mL microwave tube was placed **18d** (0.02 g, 0.97 mmol) and MeOH (2 mL), followed by 15 drops of conc H_2SO_4 . The reaction mixture was placed in a microwave reactor and heated to 90 °C with stirring for 20 min. The solution was evaporated to dryness, and the crude material was taken up in CHCl_3 and washed with a satd solution of NaHCO_3 (3 \times 50 mL). The collected organic layers were dried over anhydrous MgSO_4 , filtered, and concentrated under reduced pressure. The crude material was recrystallized from EtOH. Yield = 0.02 g (99% yield). ^1H NMR (400 MHz, CDCl_3): δ 8.99 (dd, J = 4.2, 1.7, 0.8 Hz, 1H), 8.12 (dd, J = 8.3, 1.7, 0.8 Hz, 1H), 7.89 (d, J = 8.8 Hz, 1H), 7.53 (dd, J = 8.3, 4.2 Hz, 1H), 7.27 (d, J = 1.8 Hz, 1H), 4.04 (d, J = 0.8 Hz, 3H). ESI-MS(+): m/z 437.02 $[\text{M} + \text{H}]^+$.

8,8'-Disulfanediylbis(*N*-(thiophen-2-ylmethyl)quinoline-2-carboxamide) (20). To a solution of **14b** (0.05 g, 0.24 mmol) in dry CH_2Cl_2 (2 mL) was added oxalyl chloride (0.320 mL, 2.90 mmol) and 12 drops of dry DMF under nitrogen atmosphere. The solution was stirred at room temperature for 2 h. The solution was then evaporated to dryness to remove the excess of oxalyl chloride. The resulting acyl chloride solution was then added to a solution of 2-thiophenemethylamine (0.300 mL, 2.9 mmol) in dry CH_2Cl_2 (6 mL) under nitrogen atmosphere and stirred at room temperature for 18 h. The solution was then washed with 1 M HCl to remove excess of amine, dried over anhydrous MgSO_4 , filtered, and concentrated under reduced pressure. The crude material was purified via silica gel column chromatography, eluting a gradient of 0–100% EtOAc in hexanes. Yield = 0.06 g (79%). ^1H NMR (400 MHz, CDCl_3): δ 8.59 (t, J = 6.2 Hz, 1H, NH), 8.45–8.40 (m, 1H), 8.39–8.32 (m, 1H), 7.87 (d, J = 7.6 Hz, 1H), 7.72–7.66 (m, 1H), 7.51–7.41 (m, 1H), 7.25–7.23 (m, 1H), 7.15–7.11 (m, 1H), 7.03–6.95 (m, 1H), 4.95 (d, J = 5.8 Hz, 2H). ESI-MS(+): m/z 598.93 $[\text{M} + \text{H}]^+$, 621.03 $[\text{M} + \text{Na}]^+$.

8,8'-Disulfanediylbis(*N*-benzylquinoline-2-carboxamide) (21). To a solution of **14b** (0.05 g, 0.24 mmol) in dry CH_2Cl_2 (2 mL) was added oxalyl chloride (0.042 mL, 0.48 mmol) and 5 drops of dry DMF under nitrogen atmosphere. The solution was stirred at room temperature for 2 h. The solution was evaporated to dryness to remove the excess of oxalyl chloride. The resulting acyl chloride solution was then added to a solution of benzylamine (0.319 mL, 2.9 mmol) in dry CH_2Cl_2 (5 mL) under nitrogen atmosphere, and the mixture was stirred at room temperature for 18 h. The solution was then washed with 1 M HCl to remove excess of benzylamine, dried over anhydrous MgSO_4 , filtered, and concentrated under reduced pressure. The crude material was purified via silica gel column eluting a gradient of 0–100% EtOAc in hexanes. Yield = 0.05 g (74%). ^1H NMR (400 MHz, CDCl_3): δ 8.60 (t, J = 6.2 Hz, 1H, NH), 8.43 (d, J = 8.5 Hz, 1H), 8.36 (d, J = 8.6 Hz, 1H), 7.86 (dd, J = 7.5, 1.2 Hz, 1H), 7.69 (dd, J = 8.2, 1.2 Hz, 1H), 7.49–7.43 (m, 3H), 7.40–7.34 (m, 2H), 7.30 (d, J = 7.2 Hz, 1H), 4.80 (d, J = 6.2 Hz, 2H). ESI-MS(+): m/z 587.08 $[\text{M} + \text{H}]^+$, 609.11 $[\text{M} + \text{Na}]^+$.

8,8'-Disulfanediylbis(*N*-(thiophen-2-ylmethyl)quinoline-4-carboxamide) (22). To a solution of **18d** (0.05 g, 0.24 mmol) in dry CH_2Cl_2 (2 mL) was added oxalyl chloride (0.640 mL, 5.76 mmol) and

15 drops of dry DMF under nitrogen atmosphere. The solution was stirred at room temperature for 2 h. The solution was evaporated to dryness to remove the excess of oxalyl chloride and dry CH_2Cl_2 was added to the crude material (2 mL). The resulting acyl chloride solution was added to a solution of 2-thiophenemethylamine (0.6 mL, 5.76 mmol) in dry CH_2Cl_2 (10 mL) under nitrogen atmosphere and stirred at room temperature for 2 days. The solution was then washed with 1 M HCl to remove excess of amine, dried over anhydrous MgSO_4 , filtered, and concentrated under reduced pressure. The crude material was purified via silica gel column chromatography eluting a gradient of 0–100% EtOAc in hexanes. Yield = 0.03 g (41% yield). ^1H NMR (400 MHz, $\text{DMSO}-d_6$): δ 9.47 (d, J = 5.9 Hz, 1H), 9.08 (d, J = 3.9 Hz, 1H), 7.93 (d, J = 8.4 Hz, 1H), 7.74 (d, J = 7.6 Hz, 1H), 7.67 (d, J = 4.2 Hz, 1H), 7.59–7.51 (m, 1H), 7.43 (d, J = 5.1 Hz, 1H), 7.07 (d, J = 3.3 Hz, 1H), 6.98 (s, 1H), 4.70 (d, J = 5.8 Hz, 2H). ESI-MS(+): m/z 599.05 $[\text{M} + \text{H}]^+$.

8,8'-Disulfanediylbis(N-(furan-2-ylmethyl)quinoline-4-carboxamide) (23). To a solution of **18d** (0.2 g, 0.98 mmol) in DMF (10 mL) was added carbonyldimide (CDI, 0.24 g, 1.46 mmol) and stirred at room temperature for ~15 min under nitrogen atmosphere. To this reaction mixture was added furan-2-ylmethanamine (0.146 mmol) and stirred for an additional 12 h. The resulting solution was concentrated under reduced pressure then purified via silica gel column chromatography, eluting a gradient of 0–100% EtOAc in hexanes. Yield = 0.15 g (54%). ^1H NMR (400 MHz, $\text{DMSO}-d_6$): δ 9.33 (t, J = 5.6 Hz, 1H), 9.08 (d, J = 4.4 Hz, 1H), 7.92 (d, J = 8.4 Hz, 1H), 7.76 (d, J = 7.6 Hz, 1H), 7.69–7.61 (m, 2H), 7.57 (t, J = 8.0 Hz, 1H), 6.43–6.36 (m, 2H), 4.55 (d, J = 5.6 Hz, 2H). ESI-MS(+): m/z 566.17 $[\text{M} + \text{H}]^+$.

8,8'-Disulfanediylbis(quinoline-3-carboxamide) (24). To a solution of **16b** (0.05 g, 0.24 mmol) in DMF (5 mL) was added CDI (0.06 g, 0.37 mmol) and stirred at room temperature for ~15 min under nitrogen atmosphere. To this was added NH_4OH (0.305 g, 2.44 mmol) and allowed to stir for 1 h. The resulting solution was concentrated under reduced pressure and purified via reverse-phase chromatography, eluting a gradient of 0–100% acetonitrile in H_2O . Yield = 0.016 g (32%). ^1H NMR (400 MHz, $\text{DMSO}-d_6$): δ 9.37 (d, J = 2.0 Hz, 1H), 8.91 (d, J = 2.0 Hz, 1H), 8.38 (b, 1H), 7.94 (d, J = 8.4 Hz, 1H), 7.82 (m, 2H), 7.61 (t, J = 8.0 Hz, 1H). HR-ESI-MS calcd for $[\text{C}_{20}\text{H}_{15}\text{N}_4\text{O}_2\text{S}_2]^+$, 407.0631; found, 407.0637.

8,8'-Disulfanediylbis(N-methylquinoline-3-carboxamide) (25). To a solution of **16b** (0.05 g, 0.24 mmol) in DMF (5 mL) was added hydroxybenzotriazole (HOBT, 0.06 g, 0.37 mmol) and ethyl-3-(3-(dimethylamino)propyl)carbodiimide (EDC, 0.07 g, 0.37 mmol) and stirred at room temperature for ~15 min under nitrogen atmosphere. To this reaction mixture was added methylamine (1 M THF solution, 0.49 mmol) and allowed to stir for 1 h. The resulting solution was concentrated under reduced pressure and purified via reverse-phase chromatography, eluting a gradient of 0–100% acetonitrile in H_2O . Yield = 0.018 g (34%). ^1H NMR (400 MHz, $\text{DMSO}-d_6$): δ 9.35 (s, 1H), 8.89 (m, 2H), 7.95 (d, J = 8.0 Hz, 1H), 7.83 (d, J = 8.0 Hz, 1H), 7.60 (t, J = 8.0 Hz, 1H), 2.84 (s, 3H). HR-ESI-MS calcd for $[\text{C}_{22}\text{H}_{19}\text{N}_4\text{O}_2\text{S}_2]^+$, 435.0944; found, 435.0947.

Dimethyl 2,2'-((8,8'-Disulfanediyl)bis(quinoline-8,3-diyl-3-carbonyl))bis(azanediyl)diacetate (26). To a solution of **16b** (0.04 g, 0.17 mmol) in DMF (4 mL) was added 1-[bis(dimethylamino)methylene]-1H-1,2,3-triazolo[4,5-*b*]pyridinium-3-oxidhexafluorophosphate (HATU, 0.08 g, 0.21 mmol), HOBT (0.03 g, 0.21 mmol), Et_3N (0.073 mL, 0.52 mmol), and methyl 2-aminoacetate (24 mg, 0.19 mmol) and allowed to stir at room temperature for 1 h. The resulting solution was concentrated under reduced pressure, then the crude material was then dissolved in CH_2Cl_2 and washed with 1 M HCl solution. The product, which precipitated out of the organic layer, was recrystallized from MeOH. Yield = 0.005 g (11%). ^1H NMR (400 MHz, $\text{DMSO}-d_6$): δ 9.42 (t, J = 5.9 Hz, 1H, NH), 9.37 (s, 1H), 8.93 (s, 1H), 7.97 (d, J = 8.2 Hz, 1H), 7.85 (d, J = 7.5 Hz, 1H), 7.62 (t, J = 7.7 Hz, 1H), 4.13 (d, J = 5.7 Hz, 2H), 3.68 (s, 3H). HR-ESI-MS calcd for $[\text{C}_{26}\text{H}_{23}\text{N}_4\text{O}_6\text{S}_2]^+$, 551.1054; found, 551.1052.

Procedure for the Amide Coupling (Method A). To a solution of **16b** (0.2 g, 0.98 mmol) in DMF (10 mL) was added CDI (0.24 g, 1.46

mmol) and stirred at room temperature for ~15 min under nitrogen atmosphere. To this solution was added the corresponding amine (0.146 mmol), and the solution was stirred for an additional 12 h. The resulting solution was concentrated under reduced pressure then purified via reverse-phase chromatography, eluting a gradient of 0–100% acetonitrile in H_2O .

Procedure for the Amide Coupling (Method B). To a solution of **16b** (0.2 g, 0.98 mmol) in DMF (10 mL) was added HATU (0.56 g, 1.46 mmol) and Et_3N (0.204 mL, 1.46 mmol), and the mixture was stirred at 60 °C for ~15 min under nitrogen atmosphere. To this solution was added the corresponding amine (0.146 mmol), and the solution was stirred for an additional 12 h. The resulting solution was concentrated under reduced pressure then purified via reverse-phase chromatography, eluting a gradient of 0–100% acetonitrile in H_2O .

8,8'-Disulfanediylbis(N-(oxazol-2-yl)quinoline-3-carboxamide) (27). Product afforded via method B. Yield = 0.13 g (48%). ^1H NMR (400 MHz, $\text{DMSO}-d_6$): δ 9.47 (s, 1H), 9.06 (d, J = 1.6 Hz, 1H), 8.01 (d, J = 8.0 Hz, 1H), 7.93 (s, 1H), 7.87 (d, J = 8.0 Hz, 1H), 7.64 (t, J = 8.0 Hz, 1H), 7.25 (s, 1H). HR-ESI-MS calcd for $[\text{C}_{26}\text{H}_{17}\text{N}_6\text{O}_4\text{S}_2]^+$, 541.0747; found, 541.0749.

8,8'-Disulfanediylbis(N-(thiazol-2-yl)quinoline-3-carboxamide) (28). To a solution of **16b** (0.2 g, 0.98 mmol) in DMF (10 mL) was added HATU (0.56 g, 1.46 mmol) and Et_3N (0.204 mL, 1.46 mmol), and the mixture was stirred at 60 °C for ~15 min under nitrogen atmosphere. To this solution was added the corresponding amine (0.146 mmol), and the solution was stirred for an additional 12 h. To the resulting solution was added H_2O , which resulted in the formation of a precipitate. The precipitate was isolated through vacuum filtration to afford desired product. Yield = 0.12 g (43%). ^1H NMR (400 MHz, $\text{DMSO}-d_6$): δ 9.51 (s, 1H), 9.15 (s, 1H), 7.98 (d, J = 8.0 Hz, 1H), 7.88 (d, J = 8.0 Hz, 1H), 7.64–7.59 (m, 2H), 7.32 (d, J = 2.4 Hz, 1H). ^{13}C NMR (100 MHz, $\text{DMSO}-d_6$): δ 164.5, 159.6, 149.2, 146.6, 138.2, 137.7, 135.0, 128.7, 127.8, 127.4, 127.0, 126.8, 114.7. HR-ESI-MS calcd for $[\text{C}_{26}\text{H}_{16}\text{N}_6\text{O}_2\text{S}_4\text{Na}]^+$, 595.0110; found, 595.0103.

8,8'-Disulfanediylbis(N-(tetrahydrofuran-2-yl)methyl)quinoline-3-carboxamide) (29). Product afforded via method A. Yield = 0.14 g (51%). ^1H NMR (400 MHz, $\text{DMSO}-d_6$): δ 9.43 (d, J = 2 Hz, 1H), 8.88 (d, J = 2 Hz, 1H), 7.94–7.90 (m, 3H), 7.60 (t, J = 8 Hz, 1H), 4.13–3.47 (m, 5H), 2.09–1.67 (m, 4H). HR-ESI-MS calcd for $[\text{C}_{30}\text{H}_{31}\text{N}_4\text{O}_4\text{S}_2]^+$, 575.1781; found, 575.1780.

8,8'-Disulfanediylbis(N-(furan-2-ylmethyl)quinoline-3-carboxamide) (30). Product afforded via method A. Yield = 0.084 g (30%). ^1H NMR (400 MHz, $\text{DMSO}-d_6$): δ 9.46 (d, J = 2.4 Hz, 1H), 8.99 (d, J = 2.4 Hz, 1H), 8.50 (br, 1H), 8.35 (dd, J = 7.2, 1.2 Hz, 1H), 8.28 (dd, J = 7.2, 1.2 Hz, 1H), 7.84 (t, J = 7.6 Hz, 1H), 7.50 (dd, J = 1.6, 0.8 Hz, 1H), 6.40 (m, 2H), 4.67 (d, J = 5.6 Hz, 2H). HR-ESI-MS calcd for $[\text{C}_{30}\text{H}_{22}\text{N}_4\text{O}_4\text{S}_2\text{Na}]^+$, 589.0975; found, 589.0972.

8,8'-Disulfanediylbis(N-(thiophen-2-ylmethyl)quinoline-3-carboxamide) (31). Product afforded via method A. Yield = 0.13 g (44%). ^1H NMR (400 MHz, $\text{DMSO}-d_6$): δ 9.58 (t, J = 5.6 Hz, 1H), 9.37 (d, J = 2.4 Hz, 1H), 8.91 (d, J = 2.4 Hz, 1H), 7.96 (d, J = 8 Hz, 1H), 7.84 (d, J = 8 Hz, 1H), 7.62 (t, J = 8 Hz, 1H), 7.42 (d, J = 6 Hz, 1H), 7.09–6.97 (m, 2H), 4.73 (d, J = 5.6 Hz, 2H). HR-ESI-MS calcd for $[\text{C}_{30}\text{H}_{23}\text{N}_4\text{O}_2\text{S}_4]^+$, 599.0698; found, 599.0701.

8,8'-Disulfanediylbis(N-(thiazol-2-ylmethyl)quinoline-3-carboxamide) (32). To a solution of **16b** (0.2 g, 0.98 mmol) in DMF (10 mL) was added CDI (0.24 g, 1.46 mmol) and stirred at room temperature for ~15 min under nitrogen atmosphere. To this solution was added the corresponding amine (0.146 mmol), and the solution was stirred for an additional 12 h. To the reaction mixture was added H_2O , which resulted in the formation of a precipitate. The precipitate was isolated through vacuum filtration to afford final product. Yield = 0.035 g (12%). ^1H NMR (400 MHz, $\text{DMSO}-d_6$): δ 9.83 (t, J = 5.6 Hz, 1H), 9.40 (d, J = 2 Hz, 1H), 8.95 (d, J = 2 Hz, 1H), 7.97 (d, J = 8 Hz, 1H), 7.86 (d, J = 8 Hz, 1H), 7.76 (d, J = 3.2 Hz, 1H), 7.66 (d, J = 3.2 Hz, 1H), 7.63 (t, J = 8 Hz, 1H), 4.86 (d, J = 6 Hz, 2H). HR-ESI-MS calcd for $[\text{C}_{28}\text{H}_{21}\text{N}_6\text{O}_2\text{S}_4]^+$, 601.0603; found, 601.0600.

8,8'-Disulfanediylbis(N-(2-(furan-2-yl)ethyl)quinoline-3-carboxamide) (33). To a solution of **16b** (0.2 g, 0.98 mmol) in DMF (10 mL) was added CDI (0.24 g, 1.46 mmol) and stirred at room temperature

for ~15 min under nitrogen atmosphere. To this solution was added the corresponding amine (0.146 mmol), and the solution was stirred for an additional 12 h. The reaction solution was concentrated and diluted with diethyl ether, which resulted in the formation of a precipitate. The precipitate was isolated through vacuum filtration and purified via reverse-phase chromatography, eluting a gradient of 0–100% acetonitrile in H₂O. Yield = 0.065 g (22%). ¹H NMR (400 MHz, DMSO-*d*₆): δ 9.32 (d, *J* = 2 Hz, 1H), 9.04 (t, *J* = 5.2 Hz, 1H), 8.84 (d, *J* = 2 Hz, 1H), 7.94 (d, *J* = 8 Hz, 1H), 7.83 (d, *J* = 8 Hz, 1H), 7.61–7.54 (m, 2H), 6.36 (t, *J* = 2.8 Hz, 1H), 6.21 (d, *J* = 2.8 Hz, 1H), 3.62 (q, *J* = 6 Hz, 2H), 2.96 (q, *J* = 7.2 Hz, 2H). HR-ESI-MS calcd for [C₃₂H₂₆N₄O₄S₂Na]⁺, 617.1288; found, 617.1283.

8,8'-Disulfanediylbis(N-(2-(thiophen-2-yl)ethyl)quinoline-3-carboxamide) (34). To a solution of **16b** (0.2 g, 0.98 mmol) in DMF (10 mL) was added CDI (0.24 g, 1.46 mmol) and stirred at room temperature for ~15 min under nitrogen atmosphere. To this solution was added the corresponding amine (0.146 mmol), and the solution was stirred for an additional 12 h. To the resulting solution was added H₂O, which resulted in the formation of a precipitate. The precipitate was isolated through vacuum filtration and further purified via reverse-phase chromatography using a gradient of 0–100% acetonitrile in H₂O. Yield = 0.075 g (24%). ¹H NMR (400 MHz, DMSO-*d*₆): δ 9.35 (s, 1H), 9.10 (t, *J* = 5.2 Hz, 1H), 8.87 (s, 1H), 7.95 (d, *J* = 6.4 Hz, 1H), 7.84 (d, *J* = 6.4 Hz, 1H), 7.62 (t, *J* = 5.6 Hz, 1H), 7.34–6.96 (m, 3H), 3.60 (t, *J* = 6 Hz, 2H), 3.14 (t, *J* = 6 Hz, 2H). HR-ESI-MS calcd for [C₃₂H₂₇N₄O₄S₄]⁺, 627.1011; found, 627.1013.

8,8'-Disulfanediylbis(N-(2-(thiazol-2-yl)ethyl)quinoline-3-carboxamide) (35). To a solution of **16b** (0.2 g, 0.98 mmol) in DMF (10 mL) was added CDI (0.24 g, 1.46 mmol), and the mixture was stirred at room temperature for ~15 min under nitrogen atmosphere. To this solution was added the corresponding amine (0.15 mmol), and the solution was stirred for an additional ~12 h. To the resulting solution was added H₂O, which resulted in the formation of a precipitate. The precipitate was isolated through vacuum to yield the final product. Yield = 0.18 g (57%). ¹H NMR (400 MHz, DMSO-*d*₆): δ 9.33 (s, 1H), 9.11 (t, *J* = 5.2 Hz, 1H), 8.86 (s, 1H), 7.95 (d, *J* = 8 Hz, 1H), 7.84 (d, *J* = 8 Hz, 1H), 7.74 (d, *J* = 3.2 Hz, 1H), 7.62–7.58 (m, 2H), 3.74 (q, 2H), 3.34 (t, 2H). ¹³C NMR (100 MHz, DMSO-*d*₆): δ 167.7, 163.3, 148.9, 146.3, 143.0, 136.6, 134.9, 128.6, 128.6, 127.6, 127.5, 126.3, 120.4, 40.1, 32.9. HR-ESI-MS calcd for [C₃₀H₂₅N₆O₄S₄]⁺, 629.0916; found, 629.0913.

8,8'-Disulfanediylbis(N-(pyridin-2-ylmethyl)quinoline-3-carboxamide) (36). Product afforded via method B. Yield = 0.06 g (21%). ¹H NMR (400 MHz, DMSO-*d*₆): δ 9.52 (d, *J* = 2.4 Hz, 1H), 9.07 (d, *J* = 2.4 Hz, 1H), 8.77–8.58 (m, 2H), 8.36 (dd, *J* = 7.2, 1.2 Hz, 1H), 8.32 (dd, *J* = 7.2, 1.2 Hz, 1H), 7.86–7.82 (m, 2H), 7.55 (d, *J* = 8 Hz, 1H), 7.36 (t, *J* = 6 Hz, 3H), 4.82 (d, *J* = 6 Hz, 2H). HR-ESI-MS calcd for [C₃₂H₂₅N₆O₄S₂]⁺, 589.1475; found, 589.1478.

8,8'-Disulfanediylbis(N-(pyridin-3-ylmethyl)quinoline-3-carboxamide) (37). Product afforded via method B. Yield = 0.11 g (38%). ¹H NMR (400 MHz, DMSO-*d*₆): δ 9.46 (d, *J* = 2.4 Hz, 1H), 8.98 (d, *J* = 2.4 Hz, 1H), 8.70–8.52 (m, 2H), 8.34 (dd, *J* = 7.2, 1.2 Hz, 1H), 8.27 (dd, *J* = 7.2, 1.2 Hz, 1H), 7.92 (d, *J* = 7.6 Hz, 1H), 7.83 (t, *J* = 7.6 Hz, 1H), 7.43 (dd, *J* = 7.6, 4.8 Hz, 1H), 4.73 (d, *J* = 5.6 Hz, 2H). HR-ESI-MS calcd for [C₃₂H₂₅N₆O₄S₂]⁺, 589.1475; found, 589.1477.

8,8'-Disulfanediylbis(N-(pyridin-4-ylmethyl)quinoline-3-carboxamide) (38). Product afforded via method B. Yield = 0.06 g (21%). ¹H NMR (400 MHz, DMSO-*d*₆): δ 9.88 (t, *J* = 5.6 Hz, 1H), 9.46 (d, *J* = 2.4 Hz, 1H), 9.03 (d, *J* = 2.4 Hz, 1H), 8.84–8.74 (m, 2H), 7.99 (d, *J* = 8 Hz, 1H), 7.92–7.91 (m, 2H), 7.87 (d, *J* = 8 Hz, 1H), 7.65 (t, *J* = 8 Hz, 1H), 4.80 (d, *J* = 5.6 Hz, 2H). HR-ESI-MS calcd for [C₃₂H₂₅N₆O₄S₂]⁺, 589.1475; found, 589.1477.

8,8'-Disulfanediylbis(N-benzylquinoline-3-carboxamide) (39). To a solution of **16b** (0.2 g, 0.98 mmol) in DMF (10 mL) was added HATU (0.56 g, 1.46 mmol) and Et₃N (0.204 mL, 1.46 mmol), and the mixture was stirred at 60 °C for ~15 min under nitrogen atmosphere. To this solution was added the corresponding amine (0.146 mmol), and the solution was stirred for an additional 12 h. The reaction mixture was concentrated, and the crude material was dissolved in CH₂Cl₂. The product, which precipitated out of the organic layer, was

collected via vacuum filtration. Yield = 0.03 g (42%). ¹H NMR (400 MHz, DMSO-*d*₆): δ 9.49 (t, *J* = 5.9 Hz, 1H), 9.41 (d, *J* = 2.1 Hz, 1H), 8.95 (d, *J* = 2.2 Hz, 1H), 7.94 (s, 1H), 7.86–7.81 (m, 1H), 7.61 (t, *J* = 7.8 Hz, 1H), 7.41–7.32 (m, 4H), 7.26 (t, *J* = 7.1 Hz, 1H), 4.58 (d, *J* = 5.8 Hz, 2H). HR-ESI-MS calcd for [C₃₄H₂₇N₄O₂S₂]⁺, 587.1570; found, 587.1571.

8,8'-Disulfanediylbis(N-(4-fluorobenzyl)quinoline-3-carboxamide) (40). Product afforded via method A. Yield = 0.04 g (14%). ¹H NMR (400 MHz, DMSO-*d*₆): δ 9.48 (t, *J* = 5.6 Hz, 1H), 9.39 (d, *J* = 1.6 Hz, 1H), 8.92 (d, *J* = 1.6 Hz, 1H), 7.95 (d, *J* = 8.0 Hz, 1H), 7.84 (d, *J* = 8.0 Hz, 1H), 7.61 (t, *J* = 8.0 Hz, 1H), 7.44–7.15 (m, 4H), 4.56 (d, *J* = 5.6 Hz, 2H). HR-ESI-MS calcd for [C₃₄H₂₅F₂N₄O₂S₂]⁺, 623.1382; found, 623.1384.

8,8'-Disulfanediylbis(N-(4-(trifluoromethyl)benzyl)quinoline-3-carboxamide) (41). Product afforded via method A. Yield = 0.09 g (26%). ¹H NMR (400 MHz, DMSO-*d*₆): δ 9.58 (t, *J* = 5.6 Hz, 1H), 9.40 (s, 1H), 8.94 (s, 1H), 7.96 (d, *J* = 8.0 Hz, 1H), 7.85 (d, *J* = 8.0 Hz, 1H), 7.73 (d, *J* = 8.0 Hz, 2H), 7.62–7.61 (m, 3H), 4.67 (d, *J* = 5.2 Hz, 2H). ESI-MS(+): *m/z* 723.25 [M + H]⁺. HR-ESI-MS calcd for [C₃₆H₂₄F₆N₄O₂S₂Na]⁺, 745.1137; found, 745.1141.

8,8'-Disulfanediylbis(N-(4-methoxybenzyl)quinoline-3-carboxamide) (42). Product afforded via method A. Yield = 0.15 g (47%). ¹H NMR (400 MHz, DMSO-*d*₆): δ 9.40–9.38 (m, 2H), 8.91 (d, *J* = 1.6 Hz, 1H), 7.95 (d, *J* = 8.0 Hz, 1H), 7.83 (d, *J* = 8.0 Hz, 1H), 7.62 (t, *J* = 8.0 Hz, 1H), 7.30 (d, *J* = 8.0 Hz, 2H), 6.92 (d, *J* = 8.0 Hz, 2H), 4.50 (d, *J* = 5.6 Hz, 2H), 3.72 (s, 3H). HR-ESI-MS calcd for [C₃₆H₃₀N₄O₄S₂Na]⁺, 669.1601; found, 669.1603.

8,8'-Disulfanediylbis(N-(benzo[d][1,3]dioxol-5-ylmethyl)quinoline-3-carboxamide) (43). Product afforded via method A. Yield = 0.12 g (37%). ¹H NMR (400 MHz, acetone-*d*₆): δ 9.38 (s, 2H), 9.01 (s, 1H), 8.27–8.26 (m, 2H), 7.81 (d, *J* = 7.6 Hz, 1H), 6.95 (s, 1H), 6.87–6.85 (m, 2H), 5.98 (s, 2H), 4.46 (d, *J* = 5.6 Hz, 2H). HR-ESI-MS calcd for [C₃₆H₂₇N₄O₆S₂]⁺, 675.1372; found, 675.1374.

8,8'-Disulfanediylbis(N-(4-morpholinobenzyl)quinoline-3-carboxamide) (44). Product afforded via method A. Yield = 0.18 g (50%). ¹H NMR (400 MHz, DMSO-*d*₆): δ 9.40–9.33 (m, 2H), 8.91 (s, 1H), 7.94 (d, *J* = 8.0 Hz, 1H), 7.83 (d, *J* = 8.0 Hz, 1H), 7.59 (t, *J* = 8.0 Hz, 1H), 7.26 (d, *J* = 8.0 Hz, 2H), 6.93 (d, *J* = 8.0 Hz, 2H), 4.47 (d, *J* = 5.6 Hz, 2H), 3.72 (t, *J* = 4.8 Hz, 4H), 3.05 (t, *J* = 4.8 Hz, 4H). HR-ESI-MS calcd for [C₄₂H₄₀N₆O₄S₂Na]⁺, 779.2445; found, 779.2443.

8,8'-Disulfanediylbis(N-(2-morpholinoethyl)quinoline-3-carboxamide) (45). Product afforded via method A. Yield = 0.07 g (24%). ¹H NMR (400 MHz, acetone-*d*₆): δ 9.45 (s, 1H), 8.96 (s, 1H), 8.36 (d, *J* = 8 Hz, 1H), 8.30 (d, *J* = 8 Hz, 1H), 7.86 (t, *J* = 8 Hz, 1H), 3.79–3.75 (m, 6H), 3.06 (t, *J* = 6 Hz, 2H). HR-ESI-MS calcd for [C₃₂H₃₇N₆O₄S₂]⁺, 633.2312; found, 633.2316.

Dibenzyl 2,2'-((2,2'-((8,8'-Disulfanediylbis(quinoline-8,3-diyl-3-carbonyl)bis(azanediyl)bis(acetyl)bis(azanediyl)diacetate) (46). To a solution of **16b** (0.05 g, 0.24 mmol) in dry DMF (5 mL) was added HATU (0.11 g, 0.29 mmol), HOBT (0.04 g, 0.29 mmol), Et₃N (0.068 mL, 0.48 mmol), and H₂N-Gly-Gly-Bz (0.11 g, 0.26 mmol). The reaction was stirred at room temperature for 4 h. The resulting mixture was evaporated to dryness, and the crude material was dissolved in CH₂Cl₂ and washed with 1 M HCl, H₂O, and then brine. The product, which precipitated out of the organic layer, was filtered off and dried under vacuum. Yield = 0.07 g (69%). ¹H NMR (400 MHz, DMSO-*d*₆): δ 9.40 (d, *J* = 2.1 Hz, 1H), 9.29 (t, *J* = 5.9 Hz, 1H), 8.94 (d, *J* = 2.2 Hz, 1H), 8.51 (t, *J* = 6.0 Hz, 1H), 7.96 (d, *J* = 8.0 Hz, 1H), 7.88–7.82 (m, 1H), 7.62 (t, *J* = 7.8 Hz, 1H), 7.37–7.28 (m, 5H), 5.14 (s, 2H), 4.03 (d, *J* = 5.9 Hz, 2H), 3.95 (d, *J* = 5.9 Hz, 2H). HR-ESI-MS calcd for [C₄₂H₃₇N₆O₈S₂]⁺, 817.2109; found, 817.2106.

8-Hydroxy-N-(2-(thiazol-2-yl)ethyl)quinoline-3-carboxamide (47). To a solution of 8-hydroxyquinoline-3-carboxylic acid (0.1 g, 0.529 mmol) in DMF (3 mL) was added Et₃N (0.088 mL, 0.634 mmol) and HATU (0.24 g, 0.634 mmol), then allowed to stir at room temperature for ~15 min. To this was then added 2-(thiazol-2-yl)ethan-1-amine (0.08 g, 0.634 mmol) and allowed to stir for 18 h. The resulting solution was concentrated in vacuo and purified via silica gel chromatography, eluting a gradient of 0–20% MeOH in CH₂Cl₂. Yield = 0.04 g (30%). ¹H NMR (400 MHz, DMSO-*d*₆): δ 9.35 (t, *J* = 3.6 Hz, 1H), 9.26 (s, 1H), 9.17 (s, 1H), 7.78 (d, *J* = 3.2 Hz, 1H),

7.66–7.63 (m, 3H), 7.40 (t, $J = 3.6$ Hz, 1H), 3.74 (q, $J = 5.6$ Hz, 2H), 3.36 (t, $J = 6$ Hz, 2H). HR-ESI-MS calcd for $[C_{15}H_{12}N_3O_2S]^-$, 298.0656; found, 298.0658.

8-(Methylthio)-N-(2-(thiazol-2-yl)ethyl)quinoline-3-carboxamide (48). A solution of **35** (0.1 g, 0.159 mmol) in MeOH (10 mL) was cooled down to 0 °C and placed under nitrogen atmosphere. To this was added $NaBH_4$ (0.06 g, 1.59 mmol) and allowed to stir for ~20 min. The solution was then allowed to heat up to room temperature and stirred for an additional 1 h. The resulting solution was then concentrated in vacuo, dissolved in THF (10 mL), and then added CH_3I (0.23 g, 1.59 mmol) and allowed to stir at room temperature for 1 h. This solution was then refluxed for 18 h, concentrated, and purified via silica gel chromatography, eluting a gradient of 0–90% EtOAc in hexanes. Yield = 0.23 g (22%). 1H NMR (400 MHz, $CDCl_3$): δ 9.27 (s, 1H), 8.65 (s, 1H), 7.92 (br, 1H), 7.76 (d, $J = 1.6$ Hz, 1H), 7.65 (d, $J = 7.6$ Hz, 1H), 7.56 (t, $J = 7.6$ Hz, 1H), 7.46 (d, $J = 7.6$ Hz, 1H), 7.27 (d, $J = 1.6$ Hz, 1H), 4.00 (q, $J = 5.6$ Hz, 2H), 3.39 (t, $J = 6$ Hz, 2H), 2.57 (s, 3H). HR-ESI-MS calcd for $[C_{16}H_{15}N_3OS_2Na]^+$, 352.0549; found, 352.0547.

8-Bromo-5-fluoro-2-methylquinoline (49a). A solution of 2-bromo-5-fluoroaniline (10 g, 52.6 mmol) in 6 M HCl (50 mL) and toluene (50 mL) was refluxed for ~30 min. To this was then added crotonaldehyde (6.54 mL, 79 mmol) and stirred at reflux for 18 h. The resulting solution was partitioned in a separatory funnel, and the organic layer was discarded. The remaining aqueous solution was made basic with 6 M NaOH, then extracted with EtOAc. The organic layer was then isolated and dried with $MgSO_4$ then filtered and purified via silica gel chromatography, eluting a gradient 0–10% EtOAc in hexanes to afford product as an off-white solid. Yield = 5.096 g (40%). 1H NMR (400 MHz, $CDCl_3$): δ 8.31 (d, $J = 8.4$ Hz, 1H), 7.94 (q, $J = 5.6$ Hz, 1H), 7.40 (d, $J = 8.4$ Hz, 1H), 7.07 (t, $J = 8.8$ Hz, 1H), 2.83 (s, 3H). ESI-MS(+): m/z 242.28 $[M + H]^+$.

8-Bromo-5-fluoroquinoline-2-carboxylic Acid (49b). To a solution of **49a** (2g, 8.33 mmol) in pyridine (30 mL) was added selenium dioxide (2.77 g, 24.99 mmol) and heated to reflux for 16 h. The resulting solution was then concentrated in vacuo. The crude was taken up in H_2O and heated to 70 °C for 30 min. The solution was hot filtered in order to remove excess SeO_2 byproduct and afforded product as a light-tan solid. Yield = 2.25 g (95%). 1H NMR (400 MHz, $CDCl_3$): δ 8.80 (d, $J = 8.4$ Hz, 1H), 8.38 (d, $J = 8.4$ Hz, 1H), 8.25 (q, $J = 5.2$ Hz, 1H), 7.52 (t, $J = 8.8$ Hz, 1H). ESI-MS(–): m/z 268.12 $[M - H]^-$.

5-Fluoroquinoline-2-carboxylic Acid (49c). To a solution of **49b** (2.1 g, 7.90 mmol) in MeOH (30 mL) was added 1 M NaOH (17.8 mL, 17.8 mmol) followed by $Pd(OH)_2/C$ (0.277 g, 0.395 mmol) and allowed to stir at room temperature under a hydrogen atmosphere (balloon) for 2.5 h. The resulting solution was filtered over Celite and rinsed with H_2O and MeOH. The filtrate was recovered and concentrated in vacuo to remove organic solvent. The resulting aqueous solution was then acidified with 1 M HCl to make solution slightly acidic. The acidic solution was then extracted with EtOAc. The combined organic layers were dried with $MgSO_4$ and filtered to remove solids. The filtrate was concentrated to afford product as a tan solid. Yield = 0.389 g (26%). 1H NMR (400 MHz, acetone- d_6): δ 8.74 (d, $J = 8.8$ Hz, 1H), 8.31 (d, $J = 8.4$ Hz, 1H), 8.03 (d, $J = 8.8$ Hz, 1H), 7.92 (q, $J = 6$ Hz, 1H), 7.54 (t, $J = 8$ Hz, 1H). ESI-MS(–): m/z 190.22 $[M - H]^-$.

5-Fluoro-N-(2-(thiazol-2-yl)ethyl)quinoline-2-carboxamide (49d). To a solution of **49c** (0.15 g, 0.785 mmol) in DMF (5 mL) was added Et_3N (0.131 mL, 0.942 mmol) followed by HATU (0.358 g, 0.942 mmol) and then 2-(thiazol-2-yl)ethan-1-amine (0.121 g, 0.942 mmol) and allowed to stir at room temperature for 15 h. To the resulting solution was added saturated $NaHCO_3(aq)$ and allowed to stir for ~10 min. This was then extracted with EtOAc and dried with $MgSO_4$, filtered, then concentrated and purified via silica gel chromatography, eluting a gradient of 0–50% EtOAc in hexanes. Yield = 0.1 g (42%). 1H NMR (400 MHz, $CDCl_3$): δ 8.73 (br, 1H), 8.59 (d, $J = 8.8$ Hz, 1H), 8.36 (d, $J = 8.8$ Hz, 1H), 7.91 (d, $J = 8.8$ Hz, 1H), 7.78 (d, $J = 3.2$ Hz, 1H), 7.71–7.66 (m, 1H), 7.30 (d, $J = 8.8$ Hz, 1H), 7.25 (d, $J = 3.2$

Hz, 1H), 4.02 (q, $J = 6.8$ Hz, 1H), 3.43 (t, $J = 6.8$ Hz, 1H). ESI-MS(+): m/z 302.11 $[M + H]^+$.

5-((4-Methoxybenzyl)thio)-N-(2-(thiazol-2-yl)ethyl)quinoline-2-carboxamide (49e). To a solution of **49d** (0.1 g, 0.332 mmol) in DMF (5 mL) was added p -MBSH (0.195 mL, 1.327 mmol) and NaH (0.05 g, 1.327 mmol) then allowed to stir at 140 °C for 22 h. The resulting solution was concentrated in vacuo and purified via silica gel chromatography, eluting a gradient of 0–50% EtOAc in hexanes. Yield = 0.07 g (47%). 1H NMR (400 MHz, $CDCl_3$): δ 8.73 (br, 1H), 8.59 (d, $J = 8.8$ Hz, 1H), 8.36 (d, $J = 8.8$ Hz, 1H), 7.91 (d, $J = 8.8$ Hz, 1H), 7.78 (d, $J = 3.2$ Hz, 1H), 7.71–7.66 (m, 1H), 7.30 (d, $J = 8.8$ Hz, 1H), 7.25 (d, $J = 3.2$ Hz, 1H), 4.02 (q, $J = 6.8$ Hz, 2H), 3.43 (t, $J = 6.8$ Hz, 2H). ESI-MS(+): m/z 436.13 $[M + H]^+$.

5,5'-Disulfanediylbis(N-(2-(thiazol-2-yl)ethyl)quinoline-2-carboxamide) (49f). To a solution of **49e** (0.05 g, 0.115 mmol) in TFA (5 mL) was added m -cresol (0.1 g, 0.956 mmol) and refluxed for 22 h. The resulting solution was concentrated in vacuo and purified via silica gel chromatography, eluting a gradient of 0–50% EtOAc in hexanes. Yield = 0.004 g (12%). 1H NMR (400 MHz, $DMSO-d_6$): δ 9.21 (t, $J = 6$ Hz, 1H), 8.66 (d, $J = 8.8$ Hz, 1H), 8.15 (d, $J = 8$ Hz, 1H), 8.10 (d, $J = 8.8$ Hz, 1H), 7.82–7.76 (m, 2H), 7.73 (d, $J = 3.6$ Hz, 1H), 7.59 (d, $J = 3.6$ Hz, 1H), 3.76 (q, $J = 6.8$ Hz, 2H), 3.33 (t, $J = 6.8$ Hz, 2H). HR-ESI-MS calcd for $[C_{30}H_{24}N_6O_4S_2Na]^+$, 651.0736; found, 651.0736.

Methyl 5-(((2,2-Dimethyl-4,6-dioxo-1,3-dioxan-5-ylidene)methyl)amino)nicotinate (50a). To a preheated (~100 °C) mixture of 3-aminopyridine (0.61 g, 4.0 mmol) and Meldrum's acid (0.69 g, 4.8 mmol) was added triethyl orthoformate (4.0 mL, 24.0 mmol). The mixture was stirred at 100 °C for 2 h. The reaction proceeded by changing color from yellow to wine-red accompanying the formation of yellow precipitate. After cooling to room temperature, the excess liquid of triethyl orthoformate was removed via vacuum distillation. The resulting solid was purified via silica gel chromatography, eluting a gradient of 30–70% EtOAc in CH_2Cl_2 . Yield = 1.6 g (88%). 1H NMR (400 MHz, $CDCl_3$): δ 11.32 (d, $J = 13.6$ Hz, 1H), 9.09 (s, 1H), 8.75 (s, 1H), 8.68 (d, $J = 13.6$ Hz, 1H), 8.22 (s, 1H), 3.98 (s, 3H), 1.75 (s, 6H). ^{13}C NMR (100 MHz, $CDCl_3$): δ 165.6, 164.7, 163.1, 152.8, 148.5, 144.10, 134.9, 127.2, 125.3, 105.9, 89.7, 53.1, 27.4. ESI-MS(+): m/z 306.97 $[M + H]^+$.

Methyl 8-Hydroxy-1,5-naphthyridine-3-carboxylate (50b). To a solution of **50a** (0.5 g, 1.63 mmol) was added Dowtherm A (150 mL) under nitrogen atmosphere and heated to 250 °C for 1 h. During the reaction, the color of the solution changed from orange–yellow to dark-brown. After cooling down to room temperature, the reaction solution was filtered to afford product. The solid was rinsed with diphenyl ether and acetone. Yield = 0.15 g (45%). ESI-MS(+): m/z 205.29 $[M + H]^+$.

Methyl 8-Chloro-1,5-naphthyridine-3-carboxylate (50c). To a solution of **50b** (0.1 g, 0.49 mmol) in toluene (10 mL) was added $POCl_3$ (0.14 mL, 1.47 mmol) at room temperature. The solution was stirred at 110 °C for 2 h, then allowed to cool to room temperature, which caused formation of a precipitate. The solution and dark solid was quenched with satd $NaHCO_3$ and extracted with EtOAc. The combined organic layers were dried over anhydrous Na_2SO_4 , then filtered and concentrated under reduced pressure. The residue was purified via silica gel chromatography, eluting a gradient of 20–50% EtOAc in CH_2Cl_2 . Yield = 0.078 g (71%). 1H NMR (400 MHz, $CDCl_3$): δ 9.49 (t, $J = 2.0$ Hz, 1H), 8.95 (d, $J = 2.0$ Hz, 1H), 8.86 (d, $J = 4.8$ Hz, 1H), 7.77 (d, $J = 4.8$ Hz, 1H), 3.99 (s, 3H). ^{13}C NMR (100 MHz, $CDCl_3$): δ 165.0, 151.9, 151.2, 144.3, 144.0, 143.0, 140.2, 127.3, 126.2, 53.1. ESI-MS(+): m/z 223.26 $[M + H]^+$.

8-((4-Methoxybenzyl)thio)-1,5-naphthyridine-3-carboxylic Acid (50d). To a solution of **50c** (0.18 g, 0.81 mmol) in DMF (10 mL) was added p -MBSH (0.23 mL, 1.62 mmol) and NaH (0.1 g, 2.4 mmol, 60 wt %) at room temperature. The solution was stirred for 2 h, then acidified with 1 N HCl to pH ~ 4, then concentrated under reduced pressure. The resulting residue was diluted with H_2O , and the solid was collected to give the desired product. Yield = 0.26 g (99%). 1H NMR (400 MHz, $DMSO-d_6$): δ 9.30 (s, 1H), 8.84 (d, $J = 3.2$ Hz, 1H), 8.75 (s, 1H), 7.75 (d, $J = 3.2$ Hz, 1H), 7.45 (d, $J = 6.4$ Hz, 2H), 6.92 (d, $J = 6.4$ Hz, 2H), 4.37 (s, 2H), 3.74 (s, 3H). ^{13}C NMR (125 MHz,

DMSO- d_6): δ 166.2, 159.0, 151.9, 150.9, 149.4, 143.1, 141.4, 139.2, 130.7, 128.1, 127.9, 120.5, 114.5, 55.5, 33.8. ESI-MS(+): m/z 325.07 $[M + H]^+$.

8-(4-Methoxybenzyl)thio)-N-(2-(thiazol-2-yl)ethyl)-1,5-naphthylridine-3-carboxamide (50e). To a solution of **50d** (0.25 g, 0.77 mmol) in DMF (5 mL) was added 2-(thiazol-2-yl)ethan-1-amine (0.11 g, 0.84 mmol), pyridine (0.25 mL, 3.06 mmol), HOBT (0.24 g, 1.54 mmol), and EDC (0.3 g, 1.54 mmol) at room temperature. The solution was stirred for 2 h, then concentrated under reduced pressure. The resulting residue was diluted with H₂O and extracted with EtOAc. The combined organic layers were dried over anhydrous Na₂SO₄, filtered, and concentrated. The resulting residue was purified via silica gel chromatography, eluting a gradient of 30–70% EtOAc in CH₂Cl₂. Yield = 0.17 g (51%). ¹H NMR (400 MHz, DMSO- d_6): δ 9.24 (s, 1H), 9.18 (t, J = 4.4 Hz, 1H), 8.83 (d, J = 4.0 Hz, 1H), 7.74 (d, J = 2.8 Hz, 1H), 7.72 (d, J = 4.0 Hz, 1H), 7.60 (d, J = 2.8 Hz, 1H), 7.45 (d, J = 6.8 Hz, 2H), 6.92 (d, J = 6.8 Hz, 2H), 4.36 (s, 2H), 3.74 (s, 3H), 3.72–3.66 (m, 2H), 3.34–3.29 (m, 2H). ¹³C NMR (125 MHz, DMSO- d_6): δ 167.5, 164.7, 159.0, 151.7, 150.8, 148.6, 142.8, 142.3, 141.5, 136.3, 131.0, 130.7, 127.9, 120.2, 120.1, 114.5, 55.5, 33.7, 32.7. ESI-MS(+): m/z 437.07 $[M + H]^+$.

8-Mercapto-N-(2-(thiazol-2-yl)ethyl)-1,5-naphthylridine-3-carboxamide (50f). To a solution of **50d** (0.14 g, 0.32 mmol) in TFA (20 mL) was added *m*-cresol (0.17 mL, 1.60 mmol) at room temperature. The reaction was then heated at reflux for 16 h, then concentrated under reduced pressure and diluted with the EtOAc. The solution was neutralized with satd NaHCO₃, which caused an orange–red solid to precipitate. The solid was collected via filtration and washed with H₂O and acetone to afford product. Yield = 0.087 g (86%). ¹H NMR (400 MHz, DMSO- d_6): δ 12.97 (br, 1H), 9.19 (t, J = 4.4 Hz, 1H), 9.09 (s, 1H), 8.44 (s, 1H), 7.92 (d, J = 5.2 Hz, 1H), 7.75 (d, J = 2.4 Hz, 1H), 7.62 (d, J = 2.4 Hz, 1H), 7.50 (d, J = 5.2 Hz, 1H), 3.72–3.66 (m, 2H), 3.34–3.29 (m, 2H). ¹³C NMR (125 MHz, DMSO- d_6): δ 167.4, 164.3, 147.0, 146.6, 142.8, 134.5, 133.0, 132.1, 129.1, 128.6, 120.3, 32.6. HR-ESI-MS calcd for [C₁₄H₁₂N₄OS₂Na]⁺: 339.0345; found: 339.0348.

Synthesis of [(Tp^{Me,Ph})Zn(8TQ)]. [(Tp^{Me,Ph})ZnOH] was synthesized as previously reported.⁴³ [(Tp^{Me,Ph})ZnOH] (0.1 g, 0.177 mmol) was dissolved in CH₂Cl₂ (15 mL) to yield a colorless solution. To this was added a solution of MeOH (10 mL) containing 8-mercaptoquinoline-HCl (0.035 g, 0.177 mmol) and Et₃N (25 μ L, 0.177 mmol). The colorless solution obtained a bright-yellow color. The reaction mixture was stirred for 20 h at room temperature under a nitrogen atmosphere. The reaction mixture was then concentrated in vacuo and yielded a bright-yellow solid. The solid was dissolved in minimal amount of benzene (~5 mL). Blocks were grown out of a solution of the complex in benzene diffused with pentane.

Rpn11 Activity Assay. To measure Rpn11 activity, a synthetic peptide substrate, termed Ub4-pepOG, was engineered. This substrate consists of four linear ubiquitins connected to a short peptide sequence containing a unique cysteine to which is conjugated a single Oregon Green 488 fluorophore molecule. The peptide bond between the fourth ubiquitin and the downstream peptide is cleaved by 26S proteasome in vitro, which can be observed by SDS-PAGE and fluorescent polarization measurement. The fluorescent peptide released upon cleavage of Ub4-pepOG consists of only 30 amino acids; therefore the decrease of polarization observed in fluorescence polarization assays arose mainly from deubiquitination of the peptide and could be observed even when the proteolytic activity of the 20S CP was inhibited. The fluorescence polarization assay was performed as previously described³⁷ at 30 °C in a low-volume 384 well solid black plate. Briefly, components were added to each well in the following sequence: (1) 5 μ L of inhibitor compound in buffer containing 3% DMSO or 3% DMSO in buffer as a control, and (2) 5 μ L of 26S proteasome (Enzo Life Sciences) in buffer (20 nM proteasome was preincubated with epoxomicin at room temperature for 1 h, then diluted 10-fold in 1 \times assay buffer). Substrate (5 μ L, 3 nM Ub4-pepOG) in buffer was then added to initiate the reaction. To evaluate the effects of Zn(cyclen)²⁺ on Rpn11 activity, the assay was carried out in the same manner as described with the addition of 100 μ M Zn(cyclen)²⁺ in the titration reaction. Fluorescence polarization was

measured using a plate reader with excitation at 480 nm and emission at 520 nm. To calculate the IC₅₀ of Rpn11 inhibitors, 8–12-point titration was performed for each compound up to a concentration of 100 μ M. Rpn11 activity was normalized to the DMSO control and fitted using a dose–response curve. Reported IC₅₀ values represents the average value obtained from at least three independent measurements, with the standard deviation reported as the error.

Csn5 Activity Assay. A fluorescent substrate termed SCF^{skp2}-Nedd8OG was engineered to measure Csn5 activity in vitro.³⁸ To produce this substrate, Nedd8 containing a unique N-terminal cysteine was labeled with Oregon Green 488 and then conjugated to SCF^{skp2} as previously described.⁴⁹ This assay measures the decrease in fluorescence polarization due to the decrease in apparent molecular weight of the Oregon Green fluorophore (from the ~175 kDa substrate to ~9 kDa Nedd8OG) as a result of Csn5-dependent cleavage of the isopeptide bond which links Nedd8OG to SCF^{skp2}. Assays were performed in a low-volume 384-well solid black plate comprising equal volumes of compound, substrate (SCF^{skp2}-Nedd8OG), and enzyme (Csn5). Fluorescence polarization was recorded using the same protocol as for the Rpn11 activity assay at 30 °C. IC₅₀ was calculated as described above. Reported IC₅₀ values represents the average value obtained from at least three independent measurements, with the standard deviation reported as the error.

AMSH Activity Assay. AMSH is known to selectively cleave diubiquitin linked via K63. A substrate termed DiUb^{K63}-TAMRA was purchased from Boston Biochem to assay AMSH activity in vitro. DiUb^{K63}-TAMRA was labeled with the FRET pair TAMRA/QXL. Upon AMSH cleavage, TAMRA was separated from the quencher QXL, which resulted in an increase of TAMRA fluorescence intensity, which was monitored using a fluorescence plate reader (excitation at 540 nm and emission at 590 nm). The assay was performed in a low-volume 384-well solid black plate at 30 °C and analyzed as described above. Reported IC₅₀ values represents the average value obtained from at least three independent measurements, with the standard deviation reported as the error.

BRISC Activity Assay. Purified BRISC complex (consisting of KIAA0157, BRCC-45, BRCC-36, and MERIT-40) was kindly provided by Dr. Elton Zeqiraj (University of Leeds, UK). DiUb^{K63}-TAMRA (Boston Biochem, MA) was used to measure the activity of BRISC complex. Upon cleavage, TAMRA was separated from the quencher QXL which resulted in an increase of TAMRA fluorescence intensity monitored using excitation at 540 nm and emission at 590 nm. The assay was performed in a low-volume 384-well solid black plate at 30 °C and analyzed as described above. Reported IC₅₀ values represents the average value obtained from at least three independent measurements, with the standard deviation reported as the error.

HDAC1 and 6 Activity Assay. HDAC1 and 6 were purchased from BPS Bioscience (BPS Bioscience catalogue nos. 50051 and 50006), and the assay was carried out as instructed by manufacturer. The enzyme was diluted with 25 mM Tris-Cl, 137 mM NaCl, 2.7 mM KCl, 1 mM MgCl₂, 0.1 mg/mL BSA, pH 8.0, buffer, and its activity was measured by utilizing Substrate 3 (BPS Bioscience catalogue no. 50037). The assays were carried out in black, low binding NUNC 96-well plates. Each well contained a volume of 50 μ L including buffer, HDAC (3.8 ng/well of HDAC-1, 50 ng/well of HDAC-6), inhibitor, and substrate (20 μ M). Prior to adding substrate, the plate was preincubated for 5 min. Upon addition of substrate, the plate was incubated at 37 °C for 30 min. At this point, HDAC assay developer (50 μ L, BPS Bioscience catalogue no. 50030) was added to each well and the plate was incubated for 15 min at room temperature. The fluorescence was recorded with a BioTek FLx 800 microplate reader. The measured fluorescence was compared for samples versus controls containing no inhibitor (0% inhibition). Reported IC₅₀ value represents the average values obtained from at least three independent measurements, with the standard deviation reported as the error.

MMP Activity Assay. MMP-2 and OmniMMP fluorogenic substrate (P-126) were purchased from Enzo Life Sciences (Farmingdale, NY). The assay was carried out in white NUNC 96-well plates as previously described.⁵² Each well contained a volume of

90 μL including buffer (50 mM HEPES, 10 mM CaCl_2 , 0.05% Brij-35, pH 7.5), human recombinant MMP (1.16 U of MMP-2), and the fragment solution. The enzyme and inhibitor were incubated for 30 min at 37 $^\circ\text{C}$, and the reaction was then initiated by the addition of 10 μL (100 μL total volume of wells) of the fluorogenic OmniMMP substrate (4 μM final concentration, Mca-Pro-Leu-Gly-Leu-Dpa-Ala-Arg-NH₂AcOH). Fluorescence measurements were recorded using a Bio-Tek FLx800 fluorescence plate reader every minute for 20 min with excitation and emission wavelengths at 320 and 400 nm, respectively. The rate of fluorescence increase was compared for samples versus negative controls (no inhibitor, arbitrarily set as 100% activity). Reported IC₅₀ values represents the average value obtained from at least three independent measurements, with the standard deviation reported as the error.

5-Lipoxygenase Activity Assay. The assay was performed according to a literature procedure at room temperature.⁵³ Each well contained a volume of 80 μL including buffer (50 mM Tris, 2 mM EDTA, 2 mM CaCl_2 , pH 7.5), human recombinant 5-LO (0.2 U, Cayman Chemicals), reporter dye (20, 70 -dichlorofluorescein diacetate; H₂DCFDA, 10 μM , Invitrogen), fragment solution, arachidonic acid (AA, 3 μM , Fischer Scientific), and adenosine triphosphate (ATP, 10 μM , Sigma-Aldrich). H₂DCFDA and 5-LO were incubated for 5 min prior to the addition of the fragment solution. This was followed by a second incubation for 10 min. The reaction was initiated by the addition of a substrate solution containing AA and ATP. The reaction was monitored using a Bio-Tek FLx800 fluorescence plate reader. Fluorescence measurements were recorded every minute for 20 min with excitation and emission wavelengths at 485 and 528 nm, respectively. The rate of fluorescence increase was compared for samples versus negative controls (no inhibitor, arbitrarily set as 100% activity). Reported IC₅₀ values represents the average value obtained from at least three independent measurements, with the standard deviation reported as the error.

hCAII Activity Assay. hCAII was expressed and purified as previously reported.⁵⁴ Assays were carried out in 50 mM HEPES (pH 8.0). A BioTek Precision XS microplate sample processor was utilized. The compounds were incubated with protein (final concentrations of 100 nM for hCAII) for 10 min at 25 $^\circ\text{C}$. A substrate (*p*-nitrophenylacetate; final concentration of 500 μM) was added, and hCAII-catalyzed cleavage was monitored by the increase in absorbance at 405 nm corresponding to formation of the *p*-nitrophenolate anion. The initial linear reaction rate was compared to that of wells containing no inhibitor (0% inhibition) and no protein (100% inhibition). The rate of non-hCAII-catalyzed PNPA hydrolysis in the presence of inhibitor was subtracted from each trial before determination of the percent inhibition. Reported IC₅₀ values represents the average value obtained from at least three independent measurements, with the standard deviation reported as the error.

Ub^{G76V}-GFP Degradation Assay. To determine the potency of Rpn11 inhibitor in cells, a reporter degradation assay was employed. Briefly, stably transfected HeLa cells expressing Ub^{G76V}-GFP were treated with the reversible proteasome inhibitor MG132 at 37 $^\circ\text{C}$ incubator with 5% CO₂ in air, which increased cellular levels of Ub^{G76V}-GFP to yield a detectable fluorescent signal. After 4 h, MG132 was removed and a cycloheximide (CHX) chase was initiated with or without varying concentrations of inhibitor compound at 37 $^\circ\text{C}$ with 5% CO₂ in air. Reporter degradation, monitored by the decay of GFP fluorescence, was measured to quantify Rpn11 inhibition using high throughput microscopy. The rate of fluorescence decrease was normalized to a DMSO control and analyzed using dose–response equation. Reported IC₅₀ values represents the average value obtained from at least three independent measurements, with the standard deviation reported as the error.

Cytotoxicity Assay. 293T, A549, and HCT 116 cell lines were cultured in DMEM with 10% FBS in white, clear-bottom tissue culture-treated 96-well plates. Cells were treated with different concentrations of inhibitor compounds in triplicates for 72 h at 37 $^\circ\text{C}$ with 5% CO₂ in air. CellTiter-Glo (Promega, Madison, WI) reagent was added to the 96-well plates to measure cell viability. Luminescence values were measured in PHERAstar microplate reader

(BMG labtech, Ortenberg, Germany). Collected data was normalized to DMSO control and fit to a dose–response equation to determine IC₅₀ values. Reported IC₅₀ values represents the average value obtained from at least three independent measurements, with the standard deviation reported as the error.

■ ASSOCIATED CONTENT

Supporting Information

The Supporting Information is available free of charge on the ACS Publications website at DOI: 10.1021/acs.jmedchem.6b01379.

Compound identification and molecular formula strings; inhibition of 8TQ against the BBRC36 (BRISC) complex (PDF)

Molecular formula strings (CSV)

■ AUTHOR INFORMATION

Corresponding Authors

*For S.M.C.: phone, 858-822-5596; fax, 858-822-5598; E-mail, scohen@ucsd.edu; address, Department of Chemistry & Biochemistry, University of California, San Diego, 9500 Gilman Drive, La Jolla, California 92093, United States.

*For R.J.D.: phone, 626-395-3162; E-mail, deshaies@caltech.edu; address, Division of Biology and Biological Engineering and Howard Hughes Medical Institute, California Institute of Technology, Box 114-96, Pasadena, California 91125, United States.

ORCID

Seth M. Cohen: 0000-0002-5233-2280

Present Addresses

^{||}For M.R.: Department of Chemistry, Point Loma Nazarene University, 3900 Lomaland Drive, San Diego, CA 92106

[⊥]For F.P.: Calithera Biosciences, 343 Oyster Point Boulevard #300, South San Francisco, CA 94080

[#]For T.-F.C.: Department of Pediatrics, Division of Medical Genetics, Los Angeles Biomedical Research Institute at Harbor-UCLA Medical Center, 1124 W. Carson Street, CHRC 120, Torrance, CA 90502

Author Contributions

The manuscript was written by C.P., S.M.C., and R.J.D. The compounds were designed by C.P., M.R., and S.M.C. and synthesized by C.P., M.R., and Y.M. Inhibition and cellular assays were performed by J.L., A.M., T.-F.C., and F.P..

Notes

The authors declare the following competing financial interest(s): S.M.C. is a co-founder, has an equity interest, and receives income as member of the Scientific Advisory Board for Cleave Biosciences and is a co-founder, has an equity interest, and a member of the Scientific Advisory Board for Forge Therapeutics. The terms of this arrangement have been reviewed and approved by the University of California, San Diego in accordance with its conflict of interest policies.

■ ACKNOWLEDGMENTS

We acknowledge Dr. Yongxuan Su (U.C. San Diego Molecular Mass Spectrometry Facility) for aid with HR-MS and HPLC fragment purity analysis. We acknowledge Dr. Dave P. Martin and Dr. David T. Puerta for their helpful discussions and assistance with the synthesis and characterization of the [(Tp^{Me,Ph})Zn(8TQ)] metal complex and the U.C. San Diego X-ray diffraction facilities for assistance with experiments. We also thank Dr. Elton Zeqiraj for providing purified BRISC

complex. This work was initiated with an American Recovery and Reinvestment Act (ARRA) supplement to R.J.D. (3-R01-GM065997-07S1), followed by a grant to S.M.C. and R.J.D. from the National Cancer Institute (R01-CA164803). J.L. was supported in part by a Caltech Grubstake Award and CBEA Award from Amgen. R.J.D. is an Investigator of the Howard Hughes Medical Institute and this work was supported in part by HHMI.

■ ABBREVIATIONS USED

UPS, ubiquitin-proteasome system; FBDD, fragment-based drug discovery; MBP, metal-binding pharmacophore; 8TQ, 8-thioquinoline; MM, multiple myeloma; SAR, structure-activity relationship; HTS, high-throughput screen; Tp, tris(pyrzoly)-borate; *t*-BuSH, *tert*-butylthiol; *p*-MBSH, 4-methoxyphenyl-methanethiol; HCT-116, human colorectal carcinoma cells; Ub-GFP, ubiquitinated-green fluorescent protein; CycLen, 1,4,7,10-tetraazacyclododecane; 293T, human embryonic kidney cells; A549, adenocarcinomic human alveolar basal epithelial cells

■ REFERENCES

- (1) Kyle, R. A.; Rajkumar, S. V. Treatment of Multiple Myeloma: A Comprehensive Review. *Clin. Lymphoma Myeloma* **2009**, *9* (4), 278–288.
- (2) *Survival Rates by Stage for Multiple Myeloma*; American Cancer Society: Atlanta, 2016; <http://www.cancer.org/cancer/multiplemyeloma/detailedguide/multiple-myeloma-survival-rates> (accessed September 16, 2016).
- (3) Kisselev, A. F.; van der Linden, W. A.; Overkleeft, H. S. Proteasome Inhibitors: An Expanding Army Attacking a Unique Target. *Chem. Biol.* **2012**, *19* (1), 99–115.
- (4) Moreau, P.; Richardson, P. G.; Cavo, M.; Orlowski, R. Z.; San Miguel, J. F.; Palumbo, A.; Harousseau, J. L. Proteasome Inhibitors in Multiple Myeloma: 10 Years Later. *Blood* **2012**, *120* (5), 947–959.
- (5) van der Linden, W. A.; Willems, L. I.; Shabane, T. B.; Li, N.; Ruben, M.; Florea, B. I.; van der Marel, G. A.; Kaiser, M.; Kisselev, A. F.; Overkleeft, H. S. Discovery of a Potent and Highly Beta 1 Specific Proteasome Inhibitor from a Focused Library of Urea-Containing Peptide Vinyl Sulfones and Peptide Epoxyketones. *Org. Biomol. Chem.* **2012**, *10* (1), 181–194.
- (6) Desvergne, A.; Genin, E.; Marechal, X.; Gallastegui, N.; Dufau, L.; Richy, N.; Groll, M.; Vidal, J.; Reboud-Ravaux, M. Dimerized Linear Mimics of a Natural Cyclopeptide (TMC-95A) Are Potent Non-covalent Inhibitors of the Eukaryotic 20S Proteasome. *J. Med. Chem.* **2013**, *56* (8), 3367–3378.
- (7) Geurink, P. P.; van der Linden, W. A.; Mirabella, A. C.; Gallastegui, N.; de Bruin, G.; Blom, A. E. M.; Voges, M. J.; Mock, E. D.; Florea, B. I.; van der Marel, G. A.; Driessen, C.; van der Stelt, M.; Groll, M.; Overkleeft, H. S.; Kisselev, A. F. Incorporation of Non-natural Amino Acids Improves Cell Permeability and Potency of Specific Inhibitors of Proteasome Trypsin-like Sites. *J. Med. Chem.* **2013**, *56* (3), 1262–1275.
- (8) Kawamura, S.; Unno, Y.; List, A.; Mizuno, A.; Tanaka, M.; Sasaki, T.; Arisawa, M.; Asai, A.; Groll, M.; Shuto, S. Potent Proteasome Inhibitors Derived from the Unnatural cis-Cyclopropane Isomer of Belactosin A: Synthesis, Biological Activity, and Mode of Action. *J. Med. Chem.* **2013**, *56* (9), 3689–3700.
- (9) Ozcan, S.; Kazi, A.; Marsilio, F.; Fang, B.; Guida, W. C.; Koomen, J.; Lawrence, H. R.; Sebt, S. M. Oxadiazole-isopropylamides as Potent and Noncovalent Proteasome Inhibitors. *J. Med. Chem.* **2013**, *56* (10), 3783–3805.
- (10) Gallastegui, N.; Groll, M. The 26S proteasome: Assembly and Function of a Destructive Machine. *Trends Biochem. Sci.* **2010**, *35* (11), 634–642.
- (11) Tanaka, K.; Mizushima, T.; Saeki, Y. The Proteasome: Molecular Machinery and Pathophysiological Roles. *Biol. Chem.* **2012**, *393* (4), 217–234.
- (12) Reyes-Turcu, F. E.; Wilkinson, K. D. Polyubiquitin Binding and Disassembly By Deubiquitinating Enzymes. *Chem. Rev.* **2009**, *109* (4), 1495–1508.
- (13) Koulich, E.; Li, X. H.; DeMartino, G. N. Relative Structural and Functional Roles of Multiple Deubiquitylating Proteins Associated With Mammalian 26S Proteasome. *Mol. Biol. Cell* **2008**, *19* (3), 1072–1082.
- (14) Guterman, A.; Glickman, M. H. Complementary Roles for Rpn11 and Ubp6 in Deubiquitination and Proteolysis by the Proteasome. *J. Biol. Chem.* **2004**, *279* (3), 1729–1738.
- (15) Cenci, S.; Oliva, L.; Cerruti, F.; Milan, E.; Bianchi, G.; Raule, M.; Mezghrani, A.; Pasqualetto, E.; Sitia, R.; Cascio, P. Pivotal Advance: Protein Synthesis Modulates Responsiveness of Differentiating and Malignant Plasma Cells to Proteasome Inhibitors. *J. Leukocyte Biol.* **2012**, *92* (5), 921–931.
- (16) Deshaies, R. J. Proteotoxic Crisis, the Ubiquitin-Proteasome System, and Cancer Therapy. *BMC Biol.* **2014**, *12*, 94.
- (17) McCullough, J.; Clague, M. J.; Urbe, S. AMSH is an Endosome-Associated Ubiquitin Isopeptidase. *J. Cell Biol.* **2004**, *166* (4), 487–492.
- (18) Nijman, S. M. B.; Luna-Vargas, M. P. A.; Velds, A.; Brummelkamp, T. R.; Dirac, A. M. G.; Sixma, T. K.; Bernards, R. A Genomic and Functional Inventory of Deubiquitinating Enzymes. *Cell* **2005**, *123* (5), 773–786.
- (19) Zhu, P.; Zhou, W. L.; Wang, J. X.; Puc, J.; Ohgi, K. A.; Erdjument-Bromage, H.; Tempst, P.; Glass, C. K.; Rosenfeld, M. G. A Histone H2A Deubiquitinase Complex Coordinating Histone Acetylation and H1 Dissociation in Transcriptional Regulation. *Mol. Cell* **2007**, *27* (4), 609–621.
- (20) Ambroggio, X. I.; Rees, D. C.; Deshaies, R. J. JAMM: A Metalloprotease-like Zinc Site in the Proteasome and Signalosome. *PLoS Biol.* **2003**, *2* (1), e2.
- (21) Sobhian, B.; Shao, G. Z.; Lilli, D. R.; Culhane, A. C.; Moreau, L. A.; Xia, B.; Livingston, D. M.; Greenberg, R. A. RAP80 Targets BRCA1 to Specific Ubiquitin Structures at DNA Damage Sites. *Science* **2007**, *316* (5828), 1198–1202.
- (22) Cope, G. A.; Suh, G. S. B.; Aravind, L.; Schwarz, S. E.; Zipursky, S. L.; Koonin, E. V.; Deshaies, R. J. Role of Predicted Metalloprotease Motif of Jab1/Csn5 in Cleavage of Nedd8 From Cul1. *Science* **2002**, *298* (5593), 608–611.
- (23) Sato, Y.; Yoshikawa, A.; Yamagata, A.; Mimura, H.; Yamashita, M.; Ookata, K.; Nureki, O.; Iwai, K.; Komada, M.; Fukai, S. Structural Basis for Specific Cleavage of Lys 63-Linked Polyubiquitin Chains. *Nature* **2008**, *455* (7211), 358–362.
- (24) Shrestha, R. K.; Ronau, J. A.; Davies, C. W.; Guenette, R. G.; Strieter, E. R.; Paul, L. N.; Das, C. Insights into the Mechanism of Deubiquitination by JAMM Deubiquitinases from Cocystal Structures of the Enzyme with the Substrate and Product. *Biochemistry* **2014**, *53* (19), 3199–3217.
- (25) Li, J.; Yakushi, T.; Parlato, F.; Mackinnon, A. L.; Perez, C.; Ma, Y.; Carter, K. P.; Colayco, S.; Magnuson, G.; Brown, B.; Nguyen, K.; Vasile, S.; Suyama, E.; Smith, L. H.; Sergienko, E.; Pinkerton, A. B.; Chung, T. D. Y.; Palmer, A.; Pass, I.; Hess, S.; Cohen, S. M.; Deshaies, R. J. Capzimin is a Potent and Specific Inhibitor of Proteasome Isopeptidase Rpn11. *Nat. Chem. Biol.* **2017**, in press.
- (26) Kisselev, A. F.; Goldberg, A. L. Proteasome Inhibitors: From Research Tools to Drug Candidates. *Chem. Biol.* **2001**, *8* (8), 739–758.
- (27) Adams, J. The Development of Proteasome Inhibitors as Anticancer Drugs. *Cancer Cell* **2004**, *5* (5), 417–421.
- (28) Crawford, L. J.; Walker, B.; Irvine, A. E. Proteasome Inhibitors in Cancer Therapy. *J. Cell Commun. Signal.* **2011**, *5* (2), 101–110.
- (29) Lim, H. S.; Archer, C. T.; Kodadek, T. Identification of a Peptoid Inhibitor of the Proteasome 19S Regulatory Particle. *J. Am. Chem. Soc.* **2007**, *129* (25), 7750–7751.

- (30) Lim, H. S.; Cai, D.; Archer, C. T.; Kodadek, T. Periodate-Triggered Cross-Linking Reveals Sug2/Rpt4 as the Molecular Target of a Peptoid Inhibitor of the 19S Proteasome Regulatory Particle. *J. Am. Chem. Soc.* **2007**, *129* (43), 12936–12937.
- (31) Trader, D. J.; Simanski, S.; Kodadek, T. A Reversible and Highly Selective Inhibitor of the Proteasomal Ubiquitin Receptor Rpn13 Is Toxic to Multiple Myeloma Cells. *J. Am. Chem. Soc.* **2015**, *137* (19), 6312–6319.
- (32) Anchoori, R. K.; Karanam, B.; Peng, S. W.; Wang, J. W.; Jiang, R.; Tanno, T.; Orlowski, R. Z.; Matsui, W.; Zhao, M.; Rudek, M. A.; Hung, C. F.; Chen, X.; Walters, K. J.; Roden, R. B. S. A bis-Benzylidene Piperidone Targeting Proteasome Ubiquitin Receptor RPN13/ADRM1 as a Therapy for Cancer. *Cancer Cell* **2013**, *24* (6), 791–805.
- (33) Tian, Z.; D'Arcy, P.; Wang, X.; Ray, A.; Tai, Y. T.; Hu, Y. G.; Carrasco, R. D.; Richardson, P.; Linder, S.; Chauhan, D.; Anderson, K. C. A Novel Small Molecule Inhibitor of Deubiquitylating Enzyme USP14 and UCHL5 Induces Apoptosis in Multiple Myeloma and Overcomes Bortezomib Resistance. *Blood* **2014**, *123* (5), 706–716.
- (34) Jacobsen, J. A.; Fullagar, J. L.; Miller, M. T.; Cohen, S. M. Identifying Chelators for Metalloprotein Inhibitors Using a Fragment-Based Approach. *J. Med. Chem.* **2011**, *54* (2), 591–602.
- (35) Garner, A. L.; Struss, A. K.; Fullagar, J. L.; Agrawal, A.; Moreno, A. Y.; Cohen, S. M.; Janda, K. D. 3-Hydroxy-1-alkyl-2-methylpyridine-4(1H)-thiones: Inhibition of the *Pseudomonas aeruginosa* Virulence Factor LasB. *ACS Med. Chem. Lett.* **2012**, *3* (8), 668–672.
- (36) Fullagar, J. L.; Garner, A. L.; Struss, A. K.; Day, J. A.; Martin, D. P.; Yu, J.; Cai, X. Q.; Janda, K. D.; Cohen, S. M. Antagonism of a Zinc Metalloprotease Using a Unique Metal-Chelating Scaffold: Tropolones as Inhibitors of *P. aeruginosa* Elastase. *Chem. Commun.* **2013**, *49* (31), 3197–3199.
- (37) uHTS Identification of Inhibitors of Rpn11 in a Fluorescent Polarization Assay. *PubChem BioAssay Database*; AID = 588493; National Center for Biotechnology Information: Bethesda, MD, 2012; <https://pubchem.ncbi.nlm.nih.gov/bioassay/588493> (accessed September 16, 2016).
- (38) uHTS Identification of Small Molecule Inhibitors of Csn-Mediated Deneddylation of Cullin-Ring Ligases, via a Fluorescence Polarization Assay. *PubChem BioAssay Database*; AID = 651999; National Center for Biotechnology Information: Bethesda, MD, 2013; <https://pubchem.ncbi.nlm.nih.gov/bioassay/651999> (accessed September 16, 2016).
- (39) Hopkins, A. L.; Groom, C. R.; Alex, A. Ligand Efficiency: A Useful Metric for Lead Selection. *Drug Discovery Today* **2004**, *9* (10), 430–431.
- (40) Borgneczak, K.; Tjalve, H. Effect of 8-Hydroxy-Quinoline, 8-Mercapto-Quinoline and 5-Chloro-7-Iodo-8-Hydroxy-Quinoline on the Uptake and Distribution of Nickel in Mice. *Pharmacol. Toxicol.* **1994**, *74* (3), 185–192.
- (41) Prachayasittikul, V.; Prachayasittikul, S.; Ruchirawat, S.; Prachayasittikul, V. 8-Hydroxyquinolines: A Review of Their Metal Chelating Properties and Medicinal Applications. *Drug Des., Dev. Ther.* **2013**, *7*, 1157–1178.
- (42) Su, C. Y.; Liao, S.; Wanner, M.; Fiedler, J.; Zhang, C.; Kang, B. S.; Kaim, W. The Copper(I)/Copper(II) Transition in Complexes With 8-Alkylthioquinoline Based Multidentate Ligands. *Dalton Trans.* **2003**, *2*, 189–202.
- (43) Puerta, D. T.; Cohen, S. M. Elucidating Drug-Metalloprotein Interactions with Tris(pyrazolyl)borate Model Complexes. *Inorg. Chem.* **2002**, *41* (20), 5075–5082.
- (44) Bridgewater, B. M.; Parkin, G. Lead Poisoning and the inactivation of 5-Aminolevulinic Dehydratase as Modeled by the Tris(2-mercapto-1-phenylimidazolyl)hydroborato Lead Complex, {[Tm-Ph]Pb}[ClO₄]. *J. Am. Chem. Soc.* **2000**, *122* (29), 7140–7141.
- (45) Hammes, B. S.; Carrano, C. J. Methylation of (2-Methylethanethiol-bis-3,5-dimethylpyrazolyl)methane Zinc Complexes and Coordination of the Resulting Thioether: Relevance to Zinc-Containing Alkyl Transfer Enzymes. *Inorg. Chem.* **2001**, *40* (5), 919–927.
- (46) Trofimenko, S. Recent Advances in Poly(Pyrazolyl)Borate (Scorpionate) Chemistry. *Chem. Rev.* **1993**, *93* (3), 943–980.
- (47) Tesmer, M.; Shu, M. H.; Vahrenkamp, H. Sulfur-Rich Zinc Chemistry: New Tris(thioimidazolyl)hydroborate Ligands and Their Zinc Complex Chemistry Related to the Structure and Function of Alcohol Dehydrogenase. *Inorg. Chem.* **2001**, *40* (16), 4022–4029.
- (48) Vahrenkamp, H. Transitions, Transition States, Transition State Analogues: Zinc Pyrazolylborate Chemistry Related to Zinc Enzymes. *Acc. Chem. Res.* **1999**, *32* (7), 589–596.
- (49) Duda, D. M.; Borg, L. A.; Scott, D. C.; Hunt, H. W.; Hammel, M.; Schulman, B. A. Structural Insights Into NEDD8 Activation of Cullin-RING Ligases: Conformational Control of Conjugation. *Cell* **2008**, *134* (6), 995–1006.
- (50) Chou, T. F.; Deshaies, R. J. Quantitative Cell-based Protein Degradation Assays to Identify and Classify Drugs That Target the Ubiquitin-Proteasome System. *J. Biol. Chem.* **2011**, *286* (19), 16546–16554.
- (51) Davies, C. W.; Paul, L. N.; Kim, M. I.; Das, C. Structural and Thermodynamic Comparison of the Catalytic Domain of AMSH and AMSH-LP: Nearly Identical Fold but Different Stability. *J. Mol. Biol.* **2011**, *413* (2), 416–429.
- (52) Puerta, D. T.; Griffin, M. O.; Lewis, J. A.; Romero-Perez, D.; Garcia, R.; Villarreal, F. J.; Cohen, S. M. Heterocyclic Zinc-Binding Groups for Use in Next-Generation Matrix Metalloproteinase Inhibitors: Potency, Toxicity, and Reactivity. *JBIC, J. Biol. Inorg. Chem.* **2006**, *11* (2), 131–138.
- (53) Pufahl, R. A.; Kasten, T. P.; Hills, R.; Gierse, J. K.; Reitz, B. A.; Weinberg, R. A.; Masferrer, J. L. Development of a Fluorescence-Based Enzyme Assay of Human 5-Lipoxygenase. *Anal. Biochem.* **2007**, *364* (2), 204–212.
- (54) Martin, D. P.; Hann, Z. S.; Cohen, S. M. Metalloprotein-Inhibitor Binding: Human Carbonic Anhydrase II as a Model for Probing Metal-Ligand Interactions in a Metalloprotein Active Site. *Inorg. Chem.* **2013**, *52* (21), 12207–12215.